

Chapter

Nanofibers: Production, Characterization, and Tissue Engineering Applications

Ece Bayrak

Abstract

Among all nanostructured materials, nanofibers (NFs) are the one class that is widely used in tissue engineering (TE) and regenerative medicine (RM) areas. NFs can be produced by a variety of different methods, so they can be used almost for any tissue engineering process with appropriate modifications. Also, the variety of materials that can form nanofibers, production methods, and application fields increase the value of NFs greatly. They are almost suitable for any tissue engineering applications due to their tunable properties. Hopefully, this chapter will provide brief information about the production methods (electrospinning, wet spinning, drawing, etc.), characterization methods (Scanning Electron Microscopy, Transmission Electron Microscopy, Atomic Force Microscopy, etc.), and tissue engineering applications (core-shell fibers, antibacterial fibers, nanoparticle-incorporated fibers, drug-loaded fibers, etc.) of NFs.

Keywords: nanomaterials, nanofibers, production, characterization, biomedical applications, regenerative medicine, tissue engineering

1. Introduction

Specific definition of nanofibers can vary from one discipline to another, but according to one of the most common descriptions, fibers with a diameter below 100 nm are referred as nanofibers. Nanofibers have two alike dimensions (diameter) in the nanoscale and a third dimension, which is significantly larger (length). Going back to its origins, nanofibers are produced for the first time by Formhals (1934) by electrospinning of cellulose acetate solution. Although electrospinning process was used before Formhals, no one was able to form long filaments due to the use of inelastic Newtonian fluids [1]. The use of viscoelasticity in the solutions led the formation of nanofibers because the applied electric field caused a considerable reduction of the fiber diameter due to the bending instability, which is later mentioned by Reneker [2]. Forming fibers in nanoscale was a major drawback at that time, and not much attention was paid to the topic until the breakthrough of nanotechnology in the late 1990s. After almost 60–70 years later, Formhals' work was appreciated, understood, and widened [3].

Nanofibers have many advantages because of their scales, which gave them high aspect ratio (length/diameter value) above 200 and high surface area. And because almost all their properties are tunable, one can select and use nanofibers in

numerous applications. The vital point of nanofiber technology is the availability of a wide range of materials such as natural and synthetic polymers, composites, metals, metal oxides, carbon-based materials, etc., which can be used for fiber production process [4].

Types of nanofibers can vary due to their nature, structure, and composition. According to its nature, one can produce natural or engineered nanofibers while one can produce nonporous, porous, hollow, core-shell nanofibers due to its structure. It is also possible to blend fiber materials to acquire a composition that can be organic, inorganic, carbon-based, or a composite [5]. When all the advantages considered (high aspect ratio, tunable properties, ability to form 3D networks, etc.), nanofibers are perfect nominee for different biomedical applications, such as tissue engineering (TE), regenerative medicine, drug delivery, nanoparticle delivery, etc. [6].

This chapter mainly focuses on the different production methods of nanofibers, their characterization techniques, recent developments in tissue engineering applications.

2. Nanofiber production methods

Nanofiber production techniques can be divided into two main class: top-down and bottom-up approaches. Chemical and mechanical methods are considered in top-down approaches. In top-down techniques, nanofibers are formed from bulk materials. On the other hand, in bottom-up approaches such as electrospinning, drawing, phase separation, etc., nanofiber formation occurs from composing molecules. This chapter mainly focuses on bottom-up approaches since they are the widely used class of nanofiber production methods.

2.1 Electrospinning

Electrospinning (ES) directly emerged from electrospaying (Electrohydrodynamic spray (EHD)), which was discovered by Morton and Cooley in 1902. Both methods depend on dispersing fluids by using electrostatic forces. There is one important distinction between these methods. By using ES, continuous fibers can be produced, whereas only small droplets are formed in EHD. After the electrospinning method was found to be more suitable for producing nanofibers rather than EHD, this method received more attention, and more studies were carried out in this field. As a result of these studies over the years, electrospinning method has undergone many modifications. By using different types of ES, one can produce hollow fibers, core-shell fibers, nanoparticles, or drug-incorporated fibers, etc.

2.1.1 Traditional electrospinning

For traditional ES, three main components are needed: (i) a high voltage source, (ii) syringe pump (nozzle), and (iii) a grounded collector (**Figure 1a**). The nozzle is preferably a metallic needle with a blunt tip to proper observation of the Taylor cone. During the ES process, first certain amount of polymeric solution (preferably dissolved in a volatile solvent with a w:v ratio.) is placed into a proper syringe and then to the syringe pump. Then high voltage is applied to the tip of the nozzle, and the elongating conical shape of the droplet is observed. To form nanofibers, the electrostatic force has to overcome the surface tension of the droplet, then Taylor Cone occurs at the tip of the nozzle, and a charged jet ejects from the Taylor Cone, resulting in the formation of nanofibers following by the fast evaporation of the solvent [10].

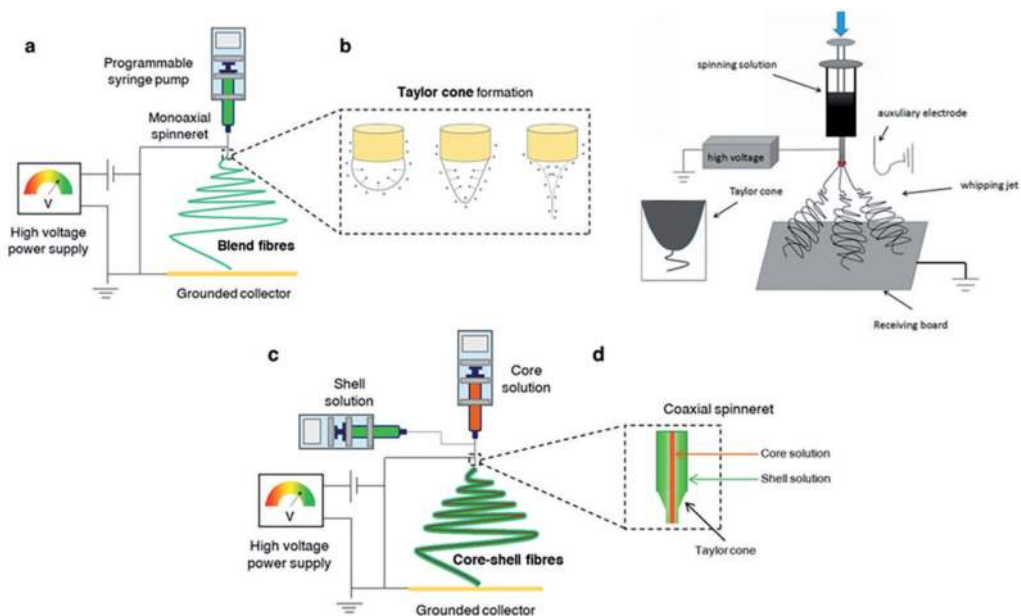


Figure 1. (a) Traditional electrospinning setup, (b) multijet electrospinning setup, and (c) coaxial electrospinning setup. (a and c were reproduced with the permission from Gonçalves et al. [7], Ura et al. [8], and b was reproduced with the permission from Wu et al. [9]).

Morphology of the formed fibers can be controlled by many factors such as flow rate of the syringe pump, concentration of the polymer solution, collector type, solution viscosity, applied voltage, distance between the collector and the nozzle, diameter of the nozzle, etc. And each of these factors affects the fiber morphology significantly. For example, by increasing the voltage, fiber diameter can be decreased, low polymer concentrations can cause electrospaying rather than electrospinning, or increasing the flow rate can reduce the fiber diameter [11]. So, all these parameters have to be optimized before the ES process began in order to obtain fibers with maximum performance.

2.1.2 Multijet electrospinning

This method is also called “Multi Needle ES” in the literature. The reason for its development is to improve the productivity and produce composite fibers that cannot be dissolved in regular solvents (**Figure 1b**).

Needle diameter, needle number, and configuration play an important role in this approach such as the other ES methods. Unfortunately, this method holds one major drawback, which is a strong repulsion among the jets because of the multi needle system. This repulsion, which is generated by the coulomb force, may cause reduced fiber deposition and poor fiber quality. To avoid this problem, needles must be oriented at appropriate distance [12].

2.1.3 Coaxial electrospinning

Coaxial ES method is used to form core-shell nanofibers by using multiple syringe pumps or one syringe pump with multiple feeding systems. Mainly, a polymer and a composite solution, one is to form shell and the other is to form core parts, can be used individually, or two different polymer solutions can be employed as forerunner solutions (**Figure 1c**). Directed by the electrostatic repulsions between the surface charges, the polymer solution, which will form the shell part

of the composite nanofibers, will be lengthened and will create viscous stress. After that this stress will be delivered to the core layer, and the polymer solution, which will form the core part, will be promptly stretched. As a result, composite jets will be formed, which will have coaxial structures [13].

2.1.4 Melt electrospinning

Addition to the conventional ES setup, melt ES technique requires a heating device such as heat guns, lasers, or electrical heating devices (**Figure 2a**). Polymer solution must stay in its molten state by a constant heat source. Main difference between melt ES and conventional ES method is the fiber formation process. In melt ES, instead of a solution, a molten polymer is used, and desired product is obtained on cooling; however, in conventional ES, fibers are formed with the help of solvent evaporation [14]. Other than this difference, the parameters that affect the fiber diameter, fiber quality, and the ES process are the same with the conventional ES method.

Main advantages of this method can be described as the absence of a solvent system and the high throughput rate of the polymer. This method can be used with the polymers that do not have a suitable solvent at room temperature. But in most of the cases, one of the major problems of melt ES is broad fiber diameter range due to the high viscosity of the melt polymer. Because of the high viscosity of the polymer, greater charge is required to initiate the jets. To reduce the fiber diameter or to obtain fibers with uniform diameters, some research groups used polymer blends or additives [17]. Requirement of high temperatures to melt the polymer can also be a disadvantage at this point. The melting temperature of the polymer can affect the structure and function of these additives (e.g., proteins, drugs, etc.) [18]. This situation makes selection and optimization steps critical.

2.1.5 Centrifugal electrospinning

Centrifugal ES is known by force spinning or rotary spinning as well. In this method, the electric field is replaced with a centrifugal force, which distinguishes centrifugal ES from conventional ES. Fiber formation is almost the same with conventional ES with a slight difference, instead of electric field, rotating speed surpasses the critical point to form a Taylor cone, and then the liquid jet gets ejected from the needle (**Figure 2b**) [19]. Therefore, rotating speed is one of the key parameters that determines the quality of the fibers along with the nozzle configuration, collector type, temperature, etc.

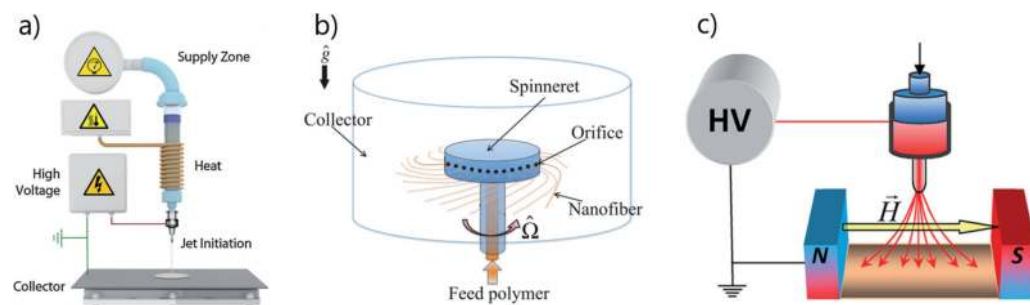


Figure 2. (a) Melt electrospinning setup, (b) centrifugal electrospinning setup, and (c) magnetic-field-assisted electrospinning setup. (a) was reproduced with the permission from Brown et al. [14]; b was reproduced with the permission from Taghavi et al. [15]; and c was reproduced with the permission from Blachowicz and Ehrmann [16]).

There are many advantages of this system due to the use of centrifugal force in place of electric field. Numerous conductive and nonconductive polymers can be electrospun with this method. Because no high voltage is needed, this method lightens safety-related concerns greatly. By adjusting the rotating speed, production efficiency can be improved, and large-scale production is allowed as well. Main limitations of conventional ES process (high voltage, misdirection of the jet, high cost, etc.) can be eliminated with this method. Aside of the advantages, the main disadvantage of this method is the spinneret design and material properties, which can highly affect the fiber quality and the yield of the process [20].

2.1.6 Magnetic-field-assisted electrospinning

In this method, magnetic properties are gained by incorporating magnetic nanoparticles to the polymer solution or using polymers that can respond to magnetic field (**Figure 2c**). This magnetic field can be obtained by two parallel permanent magnets, Helmholtz coils, or a magnetic field responder solution [21]. Besides mixing different polymers, adding non-polymeric materials (e.g., metals, ceramics, etc.) is another approach by which magnetic-field-assisted ES can be used. Fibers that are maintained with this method are reported to be more uniform. By using magnetic field fiber splitting from the jet can be prevented because of the magnetic field orientation. High velocity of the process supports smaller fiber diameter [22].

2.1.7 Needleless electrospinning

Some researchers proposed a new technique called “Needleless ES” to avoid the limitation caused by the capillaries and needles. Basis of this approach relies on a single principle, which is: Waves of an electrically conductive liquid self-organize on a mesoscopic scale and form jets when the intensity of the applied electrical field rises above a critical value (**Figure 3a**). Setup of the system can be divided in two groups: one of which is ES with a constrained feeding system and ES with an unconstrained feeding system. For the first system, a supply for the polymer solution, which is afterward injected into a closed nozzle, is preferred. On the contrary, for the second system, no nozzles are needed because the Taylor cones are formed on a free liquid surface. For both groups, high voltage source is a must to attract the polymer jets into nanofibers [25].

With the use of multiple jets without the needles, chances to increase the production rate of nanofibers are higher compared with the traditional ES systems. Some studies report an increase in polymer yield compared with single-needle

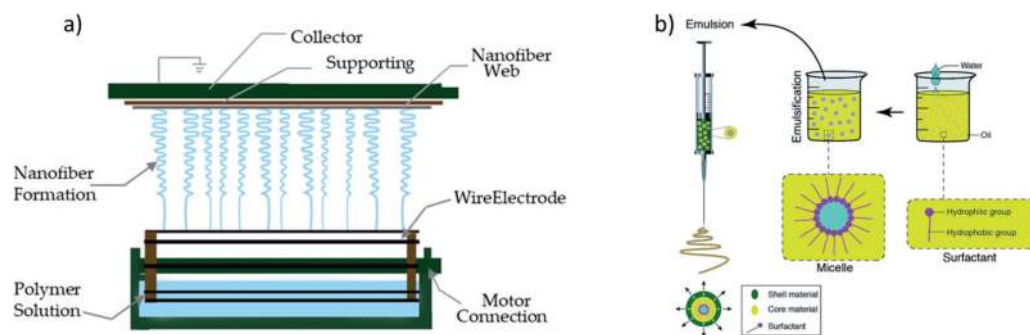


Figure 3. (a) Needleless electrospinning setup, (b) emulsion electrospinning setup. (a was reproduced with the permission from Li et al. [23], and b was reproduced with the permission from Nikmaram et al. [24]).

solution and an improvement in fiber deposition, in opposition to multi-needle ES, which resulted from a reduction in mutual fiber repulsion [26].

2.1.8 Emulsion electrospinning

Emulsion ES is developed to produce fibers from two immiscible solutions. To blend these immiscible solutions and obtain an emulsion, vigorous stirring is required. Then this emulsion is loaded a glass syringe connected to a needle and a high voltage source (**Figure 3b**). Because this emulsion contains two immiscible solutions, fibers are difficult to produce due to properties and immiscible phases of these solutions. To overcome these difficulties, nanoparticles and surfactants such as detergents, sodium dodecyl sulfate, etc., are generally used. Even with this solution, there is a constant necessity for the emulsion to stay stable through the ES process, which is a major drawback [27, 28].

2.2 Wet spinning

Wet spinning (WS) is an alternative nanofiber fabrication method for polymers that are derived from natural sources. It is much cheaper and simpler in comparison to any ES method. Because there is no high voltage source, it is much easier to load therapeutic agents into fibers, which expands the range of polymers from natural or synthetic sources handled by means of WS [29]. It is also a developing approach, but it is possible to gather wet-spun nanofibers to produce biodegradable and biocompatible scaffolds with a 3D network for regenerative medicine approaches. This method is mainly based on extrusion of a polymeric solution into a coagulation bath where the solution in the coagulation bath contains a poor solvent or solvent/non-solvent mixture (**Figure 4**).

Main goal here is to obtain coagulating fibers in the coagulation bath, which at the end solidifies as a constant fiber, as the extrusion process continues. Typical WS setup composed of a needle contains the polymeric solution, which is placed in a syringe pump and a coagulation medium. The needle must be immersed in the medium to initiate fiber coagulation. Different strategies have been developed for the collection or assembly of the fibers such as rotating drum, 3D assembly of the fibers by thermomechanical treatments, manually or computer-controlled motion of the coagulation bath or the needle, etc. After the WS setup is complete, quality and final morphology of the fibers still depend on several parameters, which include temperature, solvent system, properties of the selected polymer, needle diameter, flow rate of the syringe pump [31].

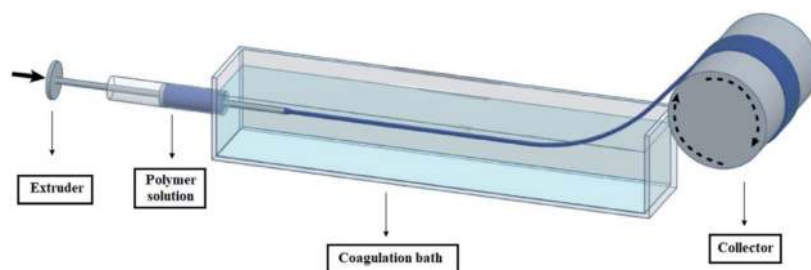


Figure 4. Wet spinning setup. (Figure was reproduced and adapted with the permission from Wang et al. [30]).

2.3 Drawing

Drawing technique is usually used to produce continuous individual nanofibers. It is based on a sharp probe tip or a micropipette, which is soaked into the edge of the droplet deposited on a container. Then the sharp tip is withdrawn from the solution with a constant rate (usually 100 $\mu\text{m/s}$) to fabricate liquid fibers. The drawn nanofibers will be deposited on the surface by contacting the surface with the edge of the micropipette (**Figure 5a**). To form a 3D structure or a network, this process was repeated several times for every droplet [33], and continuous fibers in many adjustments can be fabricated with drawing method to use in biomedical applications.

In addition, specific control of the drawing process parameters such as drawing speed, viscosity, properties of the used polymer allows repeatability of the process, control of the fiber quality and fiber dimensions. Besides the advantages such as fabricating continuous fibers, simplicity, and the cost-effectiveness of the process, there are also some limitations. Because drawing causes nanofibers to be produced one single fiber at a time, productivity of this process is low. The only material type that can be used in this process is viscoelastic materials. Viscoelastic materials can resist the increased stress produced by drawing, and they can preserve their integration while going through a strong deformation [34].

2.4 Template synthesis

Template synthesis method allows to produce solid or hollow, discontinuous nanofibers with different properties such as polymeric, metallic, ceramic, semiconductor nanofibers. It is possible to convert multiple materials into fibrils or tubules in nanoscale diameter to use them in many applications, which include regenerative medicine, electronics, optoelectronics, gas sensors, etc. [35].

This method relies on the usage of a nanoporous membrane as a template/mold, containing cylindrical pores. The template/mold often refers to a metal oxide membrane such as aluminum oxide membranes or silica-based membranes, etc. Nanofibers are formed by passing through the polymer solution from the pores of the nanoporous membrane/template (**Figure 5b**). During the extrusion, polymer

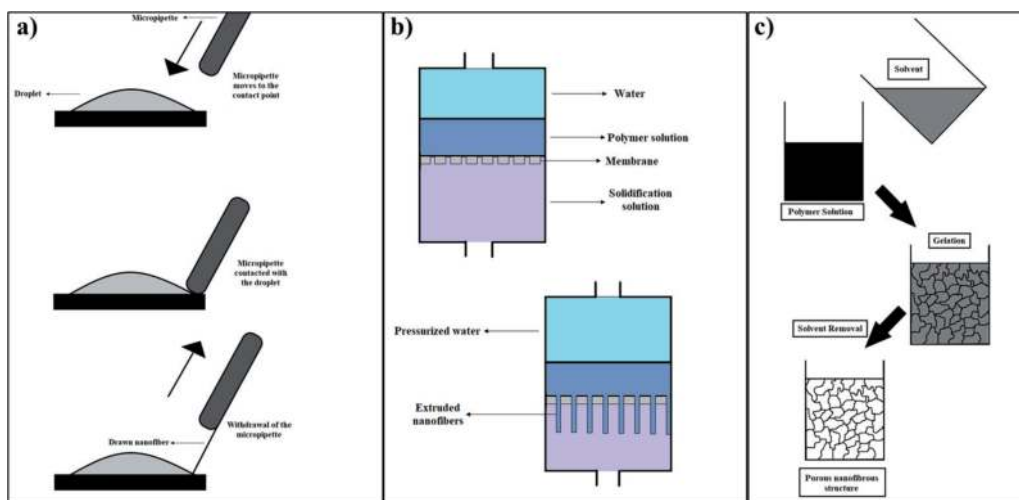


Figure 5. (a) Drawing method, (b) template synthesis method, and (c) phase separation method. (Figures were adapted from Ramakrishna et al. [32]).

solution comes in contact with the solidifying solution and nanofibers are formed. The major disadvantage of this method is the continuity of the fibers. Only a few micrometers long fibers can be obtained with this method, and the diameter of these fibers depends on the pore size of the template [36]. By using template with different pore sizes, a variety of diameters can be achieved with template synthesis.

2.5 Phase separation

Phase separation method was developed by Zhang and Ma to mimic the 3D structure of collagen under the name of thermally induced liquid-liquid phase separation (**Figure 5c**). This method is mainly composed of five stages, which include preparing a homogeneous polymer solution, phase separation process, gelation, extraction of the solvent, freezing, and freeze-drying under the vacuum. Polymer solution is often prepared by dissolving the polymer at room temperature. Then the solution reaches the gelation temperature, which is the most critical step in this method because the duration of gelation depends on the concentration of the polymer and the gelation temperature. If the polymer acquires high gelation temperature, platelet-like structures are formed due to the nucleation of crystals so low gelation temperatures are required for this process. After gelation step was completed, solvent was extracted from the gel with water, and the freeze-drying stage was applied to the final product [37, 38].

For this method, minimum equipment is needed. Nanofiber matrix can be directly fabricated, and by adjusting the polymer concentration, properties of the matrix can be accustomed. Process parameters such as polymer concentration, polymer type, solvent type, etc., were found to influence the nanofiber quality, morphology, and the final nanofibrous matrix. The matrix fabricated by the phase separation method exhibits high porosity of almost 98% within the overall material. The major drawback of this method is that only a few polymers (e.g., polylactide, polyglycolide, etc.) can be used to obtain nanofibers by phase separation due to the fact that not all polymers are compatible with this process since it requires a certain gelation capability [39].

2.6 Self-assembly

This method relies on the idea of spontaneous organization of amphiphile compounds, which can be considered as active molecules (**Figure 6**). Because self-assembly is a bottom-up fabrication method, it is based on gathering small units

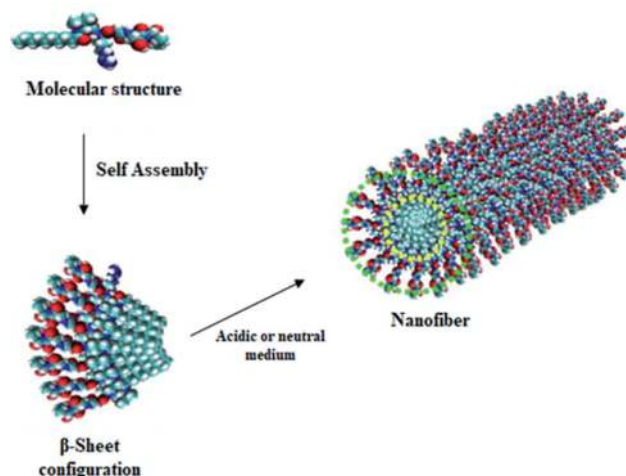


Figure 6. Self-assembly method. (Figure was adapted from Xu et al. [40]).

together by the help of intermolecular forces such as hydrogen bonding, hydrophobic interactions, electrostatic reactions, biomolecule-specific interactions, etc. These units will organize and arrange themselves to form macromolecular nanofibers.

The overall shape of the nanofibers is determined by the shape of small units. With this method, it is possible to produce nanofibers smaller than 100 nm with a length of several micrometers, but the process is time-consuming. Also, low productivity, difficult control of the fiber dimensions, and limited active compound choices, which can self-assemble themselves, are the main disadvantages of self-assembly method [41].

2.7 Interfacial polymerization

This method depends on two different monomers, which can dissolve in different phases. Basically, this is a polycondensation reaction between two reactive monomers, which are dissolved in immiscible solvents. After these two different phases are prepared and mixed, polymerization will occur at the interface of the emulsion droplet. Homogeneous nucleated growth is the key factor in interfacial polymerization [42]. By separating the monomer precursors in different phases, localized reaction and nanofiber formation can be achieved (Figure 7).

By selecting different kinds of monomers, a variety of polymers can be synthesized. The properties and quality of the nanofibers are highly dependent on the reactivity and concentration of the monomers, reactive groups attached to the monomers, and the stability of the interface [44].

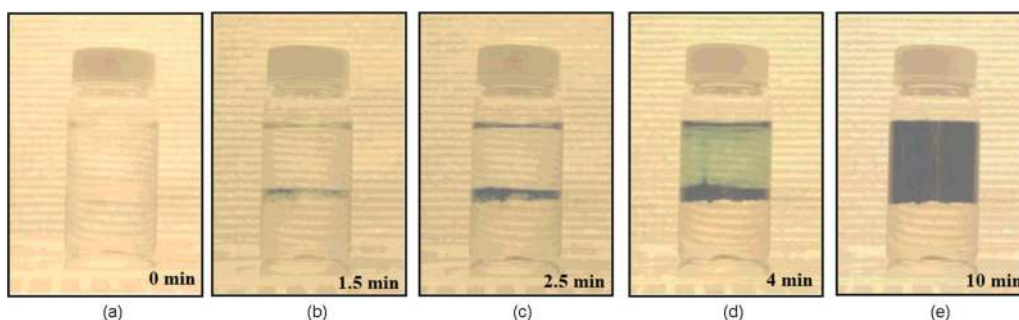


Figure 7. Snapshots showing interfacial polymerization of aniline in a water/chloroform system. From a to e, the reaction times are 0, 1.5, 2.5, 4, and 10 min, respectively. (Figure was reproduced and adapted with the permission from Huang et al. [43]).

3. Nanofiber characterization methods

Nanofibers can be produced by many different methods according to the area in which they are to be used. After choosing the appropriate production method for the application area and producing the nanofibers, some characterization studies are required to examine the quality, composition, morphology, and structure of the nanofibers. Characterization methods are still improving, and request for the establishment of effective techniques is continuously increasing. Therefore, commonly used methods for the characterization of nanofibers are described below.

3.1 Morphological and structural characterization

3.1.1 Scanning electron microscopy (SEM)

Generally, microscopic imaging techniques are routinely used to observe fiber diameters, alignment, porous structure, fiber morphology, and orientation. With

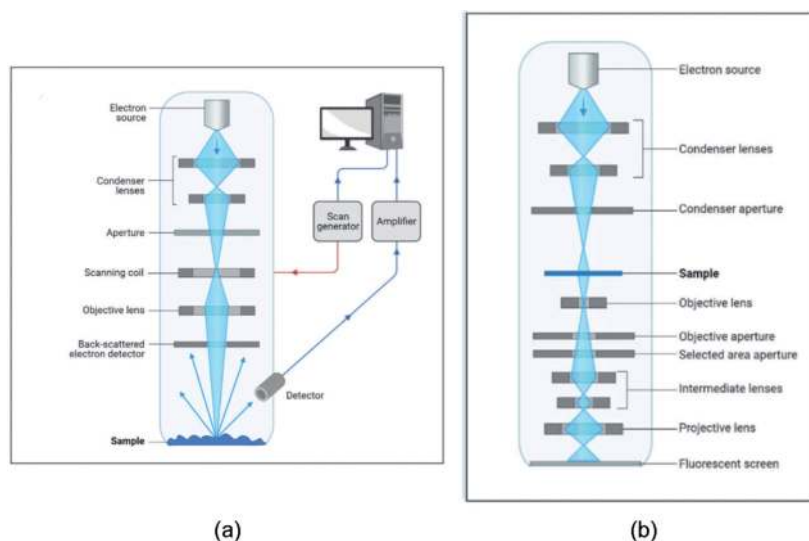


Figure 8. (a) Schematic image of scanning electron microscope, and (b) schematic image of transmission electron microscope. (Figures are reproduced from <https://biorender.com/>).

scanning electron microscopy (SEM) imaging, high-resolution images of a scaffold surface can be obtained and surface properties (roughness, porosity, smoothness, etc.) can be determined.

In order to obtain a high-resolution image from scaffolds, samples have to be conductive, so sputtering with a thin layer of a conductive metal such as gold or titanium is a common modification for nonconductive samples. After sputtering, an electron gun is used to produce beams as a cathode source and focuses by electromagnetic lenses to an exact spot on the sample. Selected spot is shaped by deflection coils so that the surface of the sample can be scanned. This procedure depends on the interaction between the beam and the secondary electrons, which are produced from the sample. Interaction between the secondary electrons from the surface of the sample and the electron beam is monitored, amplified, and illustrated in the form of an image of the surface (**Figure 8a**) [45].

For the first evaluation of the nanofiber scaffolds, SEM is the most common characterization method due to its availability and the ease of use. It is possible to determine the porosity, the width, and length of pores on the surface, which can help understand the structure of the nanofibers [46]. To analyze the qualitative characteristics of the nanofibers, a convenient number of samples are needed to obtain statistical information about the materials.

Evaluation of nanofibers, cells, living organisms, or biological materials is also possible without any coating treatment required by using environmental SEM (ESEM). In this characterization method, the electron beam is welded under water vapor environment. The ionization of water prevents the accumulation of the surface charges, which allows nonconductive materials to be evaluated without any modifications.

3.1.2 Transmission electron microscopy (TEM)

Transmission electron microscope (TEM) technology is considered one of the most important characterization techniques because of its ability to evaluate the interior structure of the samples. The pore structure of the scaffolds can be clearly seen by the images taken with TEM. The pore size and distribution of scaffolds are crucial parameters in tissue engineering field due to the fact that these parameters

directly affect the ability of the cells to penetrate through the pores of the material. Similar to SEM imaging, TEM also yields two-dimensional (2D) images of nanofibers and pores as well [45–47].

The common method includes transmitting electron beams through the ultra-thin part of the samples, which causes a phase shift in portion of the electrons. When the incoming electron beam descends from the microscope column, it interacts with the sample fluorescent screen. And then the electron beam hits the sample, which leads a large amount of radiation to be emitted from the sample. This interaction causes the elastic and inelastic scattering of the emitted electrons. Images that take origin from the elastically scattered electrons allow the observation of the structure of the scaffolds or the defects at a high resolution (**Figure 8b**). Ultrathin samples are required for TEM evaluation (~20–200 μm) because electron beams are absorbed completely by the thick samples and no image can be formed. It is a very common characterization technique, but it is also a detrimental technique as well because of the possibility to damage the samples, especially the biological samples, by the electron beam going through them [45, 46].

3.1.3 Atomic force microscopy (AFM)

Atomic force microscopy (AFM) technique is mostly used for the evaluation of surface topography. The analytical capabilities of AFM are limited to the uppermost atomic layer of a sample because its operation is based on the interactions with the electron clouds of atoms at the surface. This technique also gives information about morphology, surface roughness, fiber orientation, and particle/grain distribution from the surface of the samples [45].

In this technique, a small tip is attached to a cantilever, and when the tip encounters with the sample surface, Van der Waals and electrostatic interactions between atoms at the tip and those on the surface create a force profile and cause attraction of the tip to the surface. A photodiode detector detects the changes and converts them into data, which are later to be converted into images (**Figure 9**) [45, 49].

The operation of AFM can be carried out by three modes depending on the application: contact, noncontact, and tapping modes. The contact mode measures the repulsion between the tip and the surface of the sample where the force of the tip against sample surface remains constant. At this mode, sensitive samples can be damaged because scanning requires constant contact of the tip to the surface. The noncontact mode on the other hand measures the attractive forces between the tip

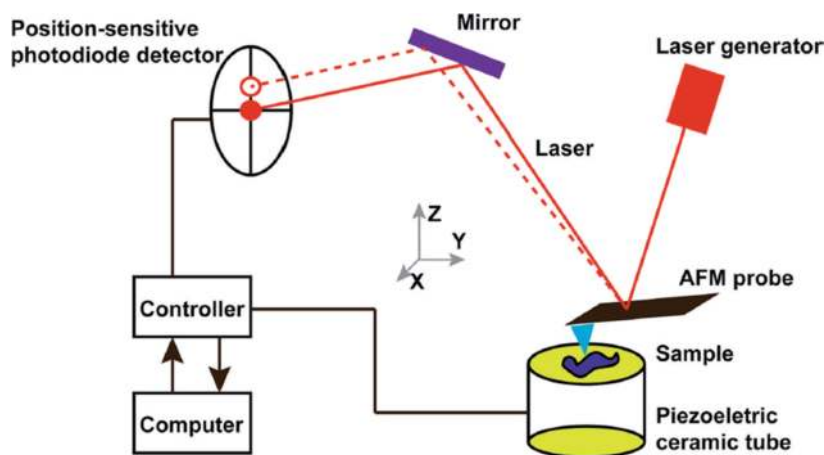


Figure 9. Atomic force microscopy setup. (Figure is reproduced with the permission from Deng et al. [48]).

and the sample surface. Van der Waals forces between the tip and the sample surface are detected. Characterization of soft materials is often made with noncontact mode. At last, the tapping mode depends on the vertical oscillation of the tip. The tip contacts the surface of the sample and then lifts off at a certain frequency. Oscillation amplitude reduces as the tip contacts the surface due to the loss of energy. This mode overcomes problems with friction, adhesion, and electrostatic forces [49].

3.1.4 X-ray diffraction (XRD)

X-ray diffraction (XRD) spectroscopy is a safe non-damaging characterization technique, which can be performed on wide range of materials such as minerals, metals, semiconductors, ceramics, polymers, etc. This technique is mostly applied to evaluate structural properties of the samples such as phase formation, crystallite size, lattice strain, contents of each phase, and crystal structure. The wavelength of X-Rays ($0.5\text{--}50 \text{ \AA}$) is similar to the distance between atoms in a solid, they are ideal for exploring atomic arrangement in crystal structure [46].

XRD, rather than measuring how the absorbance of X-rays affects the sample, examines how X-rays are diffracted from the atoms in a sample. Diffraction occurs when incident rays are scattered by atoms in a way that reinforces the waves (**Figure 10**). Working principle of XRD is basically a filament is heated to produce electrons in a cathode tube. By applying voltage, electrons are accelerated toward the sample and the sample is bombarded with electrons. Characteristic X-ray spectra are produced when electrons have enough energy to remove the inner shell electrons of the target sample. These X-rays are adjusted and located onto the sample, and the intensity of the reflected X-rays is recorded. Then these recorded signals are processed and converted to a count rate and directed to a printer or a computer monitor as an output [51].

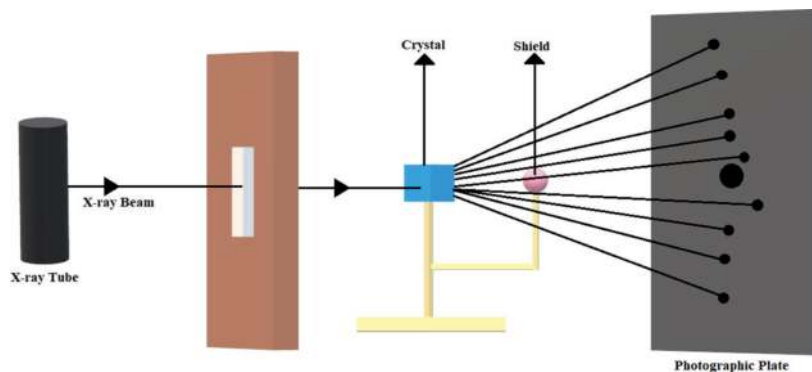


Figure 10. Working principle of X-ray diffraction. (Figure is adapted from Kaur et al. [50]).

3.1.5 Thermogravimetric analysis (TGA)

Thermal methods can be examined under two categories: (a) differential thermal analysis and (b) thermogravimetric analysis (TGA). Differential analysis depends on the changes in heat content, which is measured as a function of increasing temperature. On the other hand, thermogravimetric analysis depends on the changes in weight, which is measured as a function of increasing temperature (**Figure 11**) [53].

TGA technique relies on the use of uniform heating to decompose all organic contents at high temperature, which eventually gives information about the

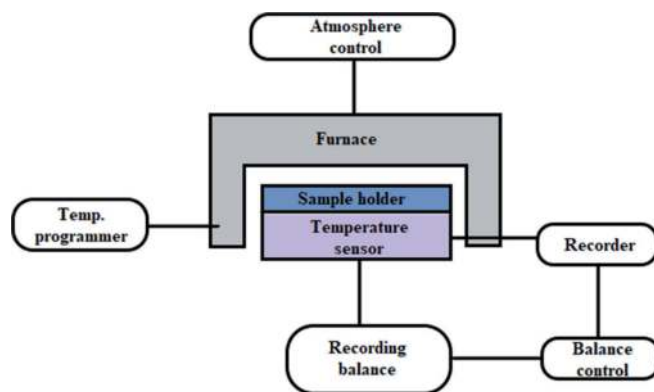


Figure 11. Thermogravimetric analysis diagram. (Figure is adapted from Loganathan et al. [52]).

compositions of the sample. Mainly, by increasing the temperature at a constant rate, the decrease in the mass of the sample is recorded. The sample is located on a balance with a platinum melting pot, which is placed inside a furnace, and the procedure is generally carried on under air gas. As a result of this analysis, mass against temperature or time plot is obtained to measure the changes in the physical and chemical properties of the sample. The obtained data provide information about thermal stability of the remained sample, dehydration, pyrolysis, solid/gas interactions, etc. [54]

3.2 Mechanical characterization

Mechanical characterization of the scaffolds plays a critical role in tissue engineering applications. The designed scaffold's mechanical properties have to match the mechanical properties of the desired tissue. The mechanical strength of a scaffolds is crucial especially for in vivo applications, where the scaffold exposed mechanical loading repeatedly.

Most common characterization technique for nanofibrous scaffolds is tensile testing or nano-tensile testing. The theory is based on the attachment of the scaffold from both sides to the grips of the tensile testing machine and then pulling the scaffold with a constant rate until the rupture occurs (**Figure 12a**). The results give information about the stress-strain values, modulus, and strength of the scaffolds. But there are two limitations, which need to be overcome. Firstly, sample gripping is a problem because fibers tend to slip from the grips or break at the grips. These machines generally are not equipped to perform under micro sizes, so the small

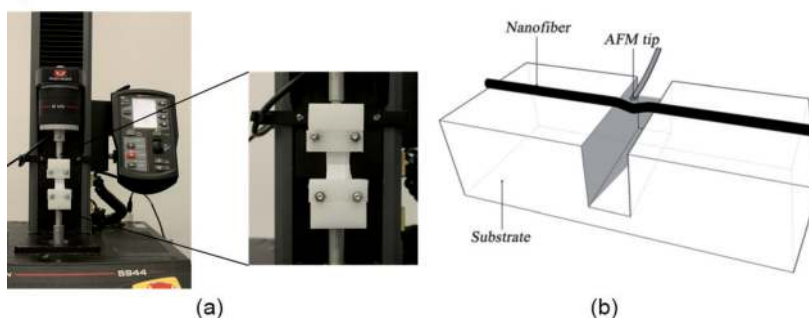


Figure 12. (a) Tensile testing of nanofiber scaffolds, and (b) nanoscale bending test schematic. (a) was author's unpublished thesis images, b was reproduced with the permission from Zhou et al. [55]).

size of the specimen is a major limitation for this process. Second, alignment of the scaffolds is needed because randomly oriented fibers may lead to premature sample failure due to unwanted bending caused by misalignment [56].

Another characterization technique that is widely used is bending test for nanofibers (nanoscale three-point bending test). The capability of an AFM system to apply forces in the nano/pico-Newton range and measure the deformation in the range of Angstroms has made this characterization method very useful. The nanofiber sample is produced or deposited on a substrate with holes in it. Then the nanofiber is positioned such that a part of it is suspended over a hole. The adhesion between the sample and the substrate is enough for the test to be performed without a failure (**Figure 12b**). With three-point bending test, Young modulus and fracture strength can be obtained. The downside of this method is that it is only limited to samples that can be produced using AFM anodization [45, 56].

3.3 Chemical characterization

3.3.1 X-ray photoelectron spectroscopy (XPS)

X-ray photoelectron spectroscopy (XPS) technique is one of the most powerful characterization techniques because of the ability of giving chemical information about the surface of the material, both elemental and molecular composition (**Figure 13a**). It can also differentiate chemical states of the same element to determine their depth distribution at a thickness between 5 and 10 nm. Useful electron signal is obtained only from a depth around 10–100 Å on the surface. Basically, the surface is irradiated by hitting the core electrons of the atoms. X-ray absorption causes the removal of an electron from one of the innermost atomic orbitals, and the kinetic energy of the emitted electron is recorded. The recorded kinetic energy is then converted into a spectrum by a computer. Binding energies of the elements from the sample will be determined according to the peaks from the spectrum. In literature, the kinetic energy and binding energy values assigned to each element can be found. This method often requires an argon ion bombardment step to eliminate surface impurities [45, 59].

3.3.2 Fourier's transform infrared spectroscopy (FTIR)

Fourier's transform infrared spectroscopy (FTIR) is a technique used to collect an infrared spectrum of an emission or an absorption of a solid, liquid, or gas. It is used to identify organic, inorganic, and polymeric materials utilizing IR light to

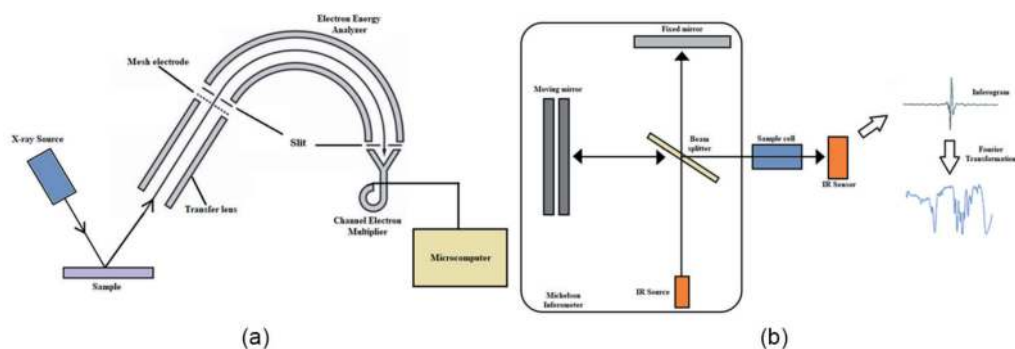


Figure 13. (a) Working principle of X-ray photoelectron spectroscopy, and (b) schematic of Fourier's transform infrared spectroscopy. (a was adapted from Seyama et al. [57], b was adapted from Lee et al. [58]).

scan samples. Standard FTIR setup is composed of a source, sample cell, detector, amplifier, A/D converter, and a computer (**Figure 13b**).

IR radiation is passed through the sample, and the emitted radiation could be absorbed and/or transmitted from the sample. Changes in the patterns of the absorption bands pinpoint a change in the composition of the material. So, the obtained signals are amplified, changes got detected by the detector, converted by the A/D converter, and as a result, a spectrum will be obtained. The obtained spectrum provides information about chemical composition of the material because the wavelength of absorbed light indicates characteristics of the chemical bonds. Just like fingerprints, two individual molecular structures cannot generate same IR spectrum. Every molecule has a specific fingerprint, which makes this technique a valuable tool for chemical identification. Also, this feature makes FTIR very preferable for many analyses such as determining the components in a mixture, identifying unknown materials, detecting contaminants in a material, finding additives, or determining the quality of a sample [60].

3.3.3 Raman spectroscopy (RS)

Raman spectroscopy (RS) method is based on irradiating a sample with a powerful laser source consisting of a monochromatic beam and measuring the scattered beam from a specific angle. During light scattering, the energy of most of the scattered light becomes equal to the energy of light interacting with the specimen. This type of elastic scattering is called Rayleigh scattering. In addition to elastic scattering, if a small part of the scattered light includes inelastic scattering, it is called Raman scattering. In Raman scattering, the excess or decrease in the energy of the scattered light relative to the energy of the light interacting with the molecule is as much as the energy difference between the energy levels of the molecule interacting with the light. This excess or scarcity at the energy levels is called the Raman shift. These shifts are measured in Raman spectroscopy (**Figure 14**) [62].

This method is used to evaluate vibrational and rotational frequency modes in physical and chemical systems. The intensity of Raman scattering depends on the change in polarizability. RS is suitable for the qualitative and quantitative analysis of organic, inorganic, and biological systems. With the obtained spectrum, unknown material identification, material differences, crystallinity, and material amount can be determined [60].

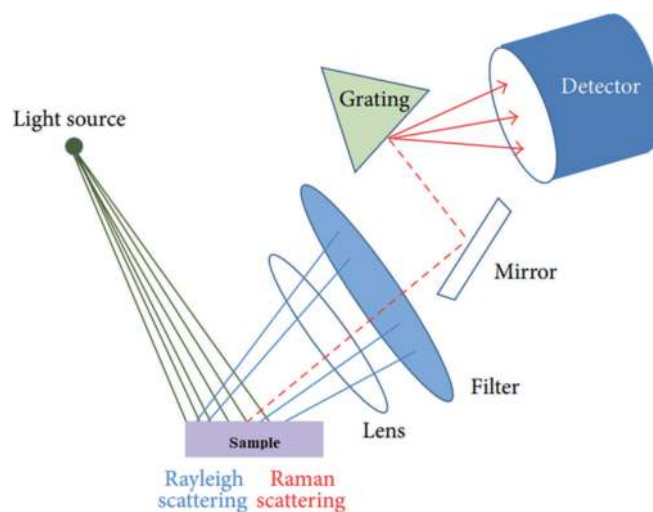


Figure 14. Working principle of Raman scattering. (Figure was adapted from Kim [61]).

4. Tissue engineering applications

As mentioned in the introduction section, natural and synthetic fibers from different sources have been widely used in many areas for hundreds of years, and tissue engineering area happens to be one of them. TE maintains an alternative way to the restoration and regeneration of the injured tissues. TE is an interdisciplinary field that requires knowledge of biological, chemical, and engineering sciences toward the objective of tissue regeneration using cells, factors, and biomaterials alone or in combination with each other. With the light of this brief information, widely used TE applications of nanofibers are discussed below.

4.1 Musculoskeletal tissue engineering applications

4.1.1 Bone tissue engineering (BTE)

Bone tissue is mainly composed of organic bone matrix, which mostly includes collagen fibers (95% of these fibers are collagen type I) and inorganic compounds such as hydroxyapatite crystals [63]. There is a global need for bone grafts because of the high incidence of bone defects, which are caused by bone tumors, infections, and bone loss by traumas. Main treatment approaches for these injuries are autografts, allografts, or xenografts. But there are some challenges to these approaches such as inflammation, scarring, infection, immunological graft rejection, hematomas, high-cost procedures, etc. [64, 65] At this point, bone tissue engineering (BTE) approaches present an alternative treatment way for these injuries. BTE field aims to form materials that can outperform bone autografts and allografts. The ultimate goal is to manufacture a scaffold that can be implanted to the defect area and then remodeled by patient's own cells. The key is to fulfill the role of the extracellular matrix (ECM) in the defect area. The design of the scaffolds for BTE is also modeled by the structure and function of healthy bone tissue, which is crucial to its function, for example, highly porous trabecular bone or highly dense cortical bone, which surrounds the trabecular bone. But still, regardless of recent advancements in TE and RM, reconstruction of critical-size bone injuries is still challenging [66].

For bone tissue regeneration, wide range of biomaterials can be used to mimic the function, structure, and composition of bone ECM with proper osteogenic activity. First studies for stimulating bone regeneration were done by ES of widely used polymers such as polycaprolactone (PCL), polylactic acid (PLA), gelatin, silk, and chitosan. The common feature of all these polymers was biodegradability because if the scaffolds are not biodegradable, a second surgery is necessary to remove the scaffold, which can result in infection, patient discomfort, or additional costs. According to the study of Cai et al., a 3D PCL/PLA scaffold was produced, and its bone regeneration efficiency was investigated in a rabbit tibia bone defect model by using human embryonic stem cell-derived mesenchymal stem cells (hESC-MSCs) [67]. They reported that the attachment of the hESC-MSCs to the 3D scaffold was successful due to the differentiation of the cells from round-like shape to a spindle-like form. Additionally, the histology and radiography studies resulted in 3D bone tissue formation after 6 weeks. Another study conducted by Nedjari, et al. is based on the development of a novel 3D honeycomb-shaped scaffold made by electrospun hybrid nanofibers, which includes poly(l-lactide- ϵ -caprolactone) and bone ECM protein fibrinogen (FBG) (**Figure 15**) [68].

Results of this study indicate that PLCL/FBG scaffolds support osteogenic differentiation of human adipose-derived mesenchymal stem cells (hADMSCs). Besides ES, melt ES writing is a promising method to design scaffolds with controlled structure. Abdalhay et al. manufactured PCL/HAp composite 3D

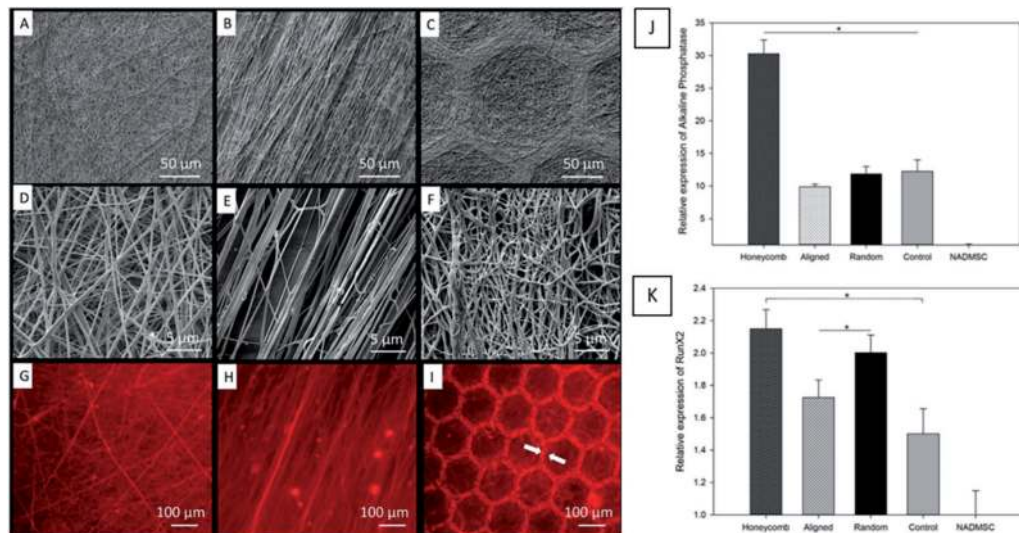


Figure 15. SEM images of random (A, D), aligned (B, E) and honeycomb (C, F) PLGL-FBG nanofibers. Bottom row represents the immunofluorescent imaging of FBG within the fibers (red) on random (G), aligned (H), and honeycomb (I)-shaped scaffolds (the arrows indicate the higher accumulation of FBG at the walls of the honeycomb shapes.). Relative expression of alkaline phosphatase gene (J) and RunX2 gene (K) of ADMS cultured for 21 days in osteogenic medium on different shaped scaffolds. (Figure was reproduced with the permission of Nedjari et al. [68]).

scaffolds with high porosity (96–98%) by using melt ES writing method [69]. According to the results, infiltration and proliferation of seeded osteoblasts were achieved, which supports high interconnectivity and porosity of the PCL/HAp scaffolds. Velioglu et al. fabricated 3D-printed PLA scaffolds with different pore sizes for trabecular bone repair and regeneration. Their findings showed that the resemblance between 3D-printed scaffolds and native trabecular bone in terms of pore size, porosity, and mechanical properties of the scaffolds, the 3D-printed PLA scaffolds printed in this study can be considered as candidates for bone substitutes in bone repair [70]. In 2019, Lukasova et al. produced 3D and 2D nanofibrous scaffolds by using centrifugal ES and needleless ES methods, respectively. Cyclone device was used as a spinneret for centrifugal ES, and the spin guidance was sideways. Needleless ES on the other hand was performed by using Nanospider® technology. Scaffolds were then tested for metabolic activity, cell differentiation, and proliferation by using hMSCs. Scaffolds obtained with centrifugal ES showed higher cell proliferation due to their 3D, porous, and interconnective architecture [71].

4.1.2 Tendon/ligament tissue engineering

Tendon/ligament injuries, which are caused by tears, ruptures, traumas, and inflammation, result in severe pain and are generally seen in physically active young patients. Natural healing of these tissues is challenging due to their poor healing capacity and scar tissue formation, which then result in poor mechanical properties. Standard treatment approaches for these injuries are grafts or artificial prosthesis. Autografts are considered “gold standard” because of their lack of immune response, but they are limited by donor site availability and morbidity. Allografts hold the same concerns as in BTE, which are rejection, risk of disease transmission, and high re-rupture rates caused by mismatches between the donor and the recipient. To overcome these challenges, TE approaches are widely used for tendon/ligament tissue repair [72].

These soft tissues are mainly composed of dense and aligned collagen fibers, so the mechanic load of tendons and ligaments is restricted to one direction. As a result, scaffolds composed of aligned nanofibers are highly promising for tendon/ligament tissue repair studies because they can mimic the anisotropic nature of the native tissues. In the light of these information, a novel, multilayer scaffold was proposed by Yang et al., which was composed of fibrous PCL and methacrylated gelatin produced by dual ES [73]. The scaffold was formed by five sheets, which were cross-linked. The scaffold was then reinforced with gelatin layer bearing the stem cells, which were treated with TGF- β 3 for 7 days to stimulate differentiation. Results showed an increase of tendon markers tenascin-C and scleraxis, which implies the scaffolds were porous enough for the diffusion of bioactive molecules. Another study conducted by Perikamana et al. reported that immobilization of platelet-derived growth factor (PDGF) in a gradient scaffold, which is also composed of aligned nanofibers, enhanced the expression of tenomodulin compared with a non-modified nanofiber scaffold [74]. Rinoldi et al., fabricated a bead-on-string fibrous

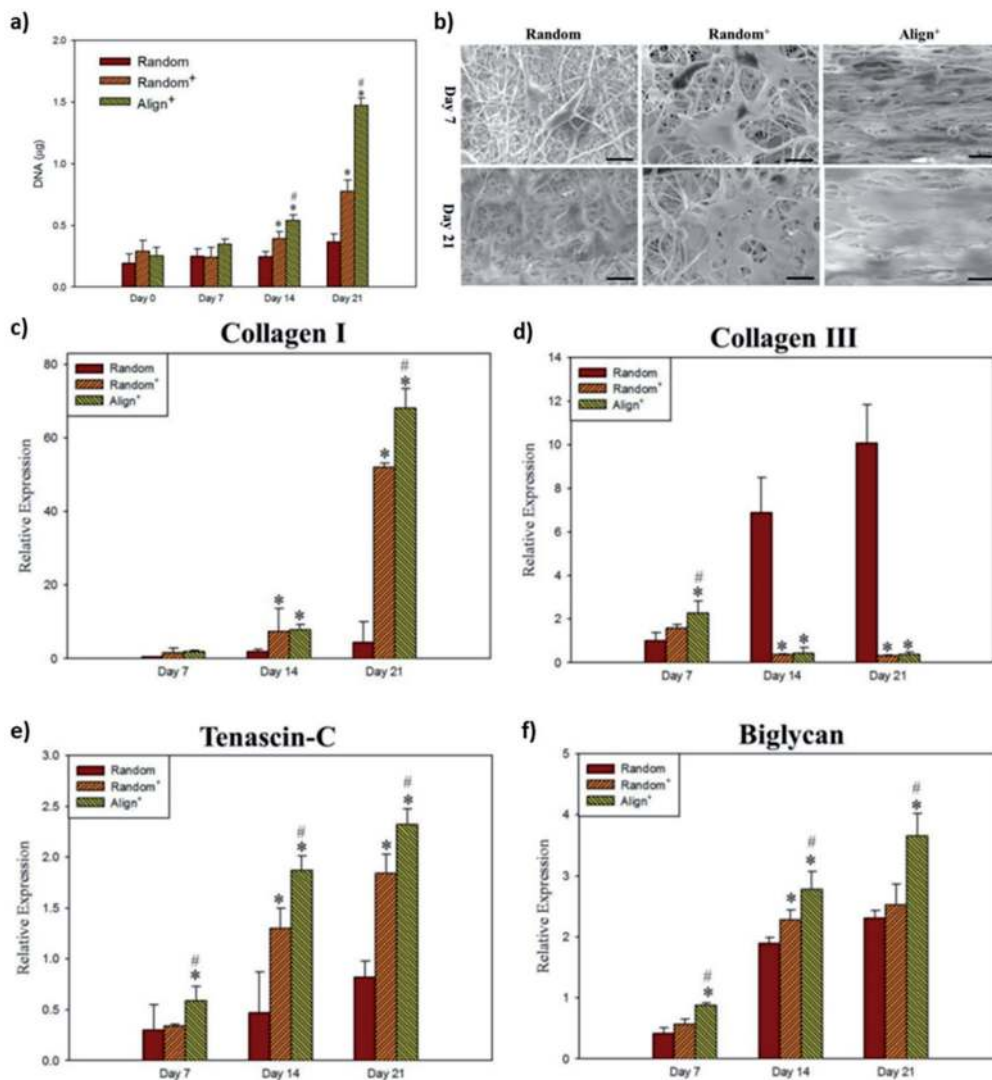


Figure 16.

The cell proliferation rates from DNA assays (a) and SEM images (b) of tenocytes cultured on different core-shell nanofiber scaffolds. The relative mRNA expression of type-I collagen (c), type III collagen (d), tenascin-C (e), and biglycan (f) by tenocytes after cultured on different core-shell nanofiber scaffolds for 7, 14, and 21 days. (Figures are reproduced with the permission from Chen et al. [76]).

scaffold and incorporated with silica particles to enhance the biological activities and modify the properties of the scaffolds such as wettability, degradation rate, etc. The results imply that their bead-to-string fibrous scaffold is a significant candidate for guided tissue regeneration [75]. In a recent study, Chen et al. proposed a three types of core-shell nanofibrous scaffolds [76]. For one group, HA (hyaluronic acid) is the core and PCL (random) is the shell while the other groups are HA/PRP (platelet-rich plasma) core-PCL shell (Random⁺) and HA/PRP core-PCL shell (Align⁺) (**Figure 16**). Tenocytes were used in in vitro studies, and the cells in Align⁺ showed the highest cell proliferation rate while Random⁺ is also significantly higher than Random study group. According to the expression studies, by day 14, Random⁺ and Align⁺ showed significant downregulation of collagen III gene expression when shift of collagen III to collagen I occurs during the tendon maturation.

It is safer to study tendon/ligament tissue regeneration compared with tendon/ligament-bone interface regeneration, which is also called the enthesis. Regeneration enthesis is exceptionally challenging due to its complex and gradient structure. The enthesis possesses location-dependent changes such as gradients, in terms of composition of ingredients and structural properties.

Still, there are many studies and research groups trying to fabricate scaffolds to repair tissue-tissue interfaces by incorporating bone-like biomaterials such as hydroxyapatite, hyaluronan, etc. (**Figure 17**) [74, 77]. Yet still, it remains a challenge in the field, which requires much more time and effort.

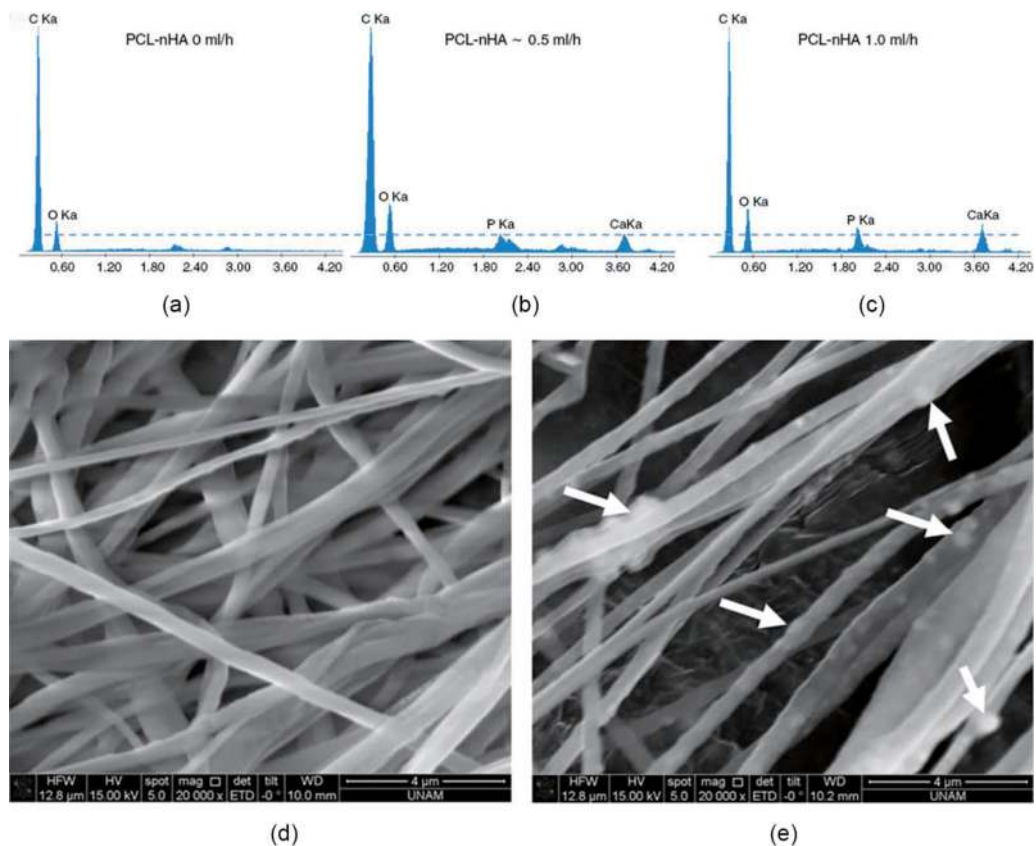


Figure 17. Energy-dispersive spectroscopy (EDS) spectrum of polycaprolactone (PCL)-only and PCL-nano-hydroxyapatite (nHA) meshes at different flow rates corresponding to different nHA concentrations (a–c). Representative scanning electron microscopy (SEM) micrographs taken from (d) polycaprolactone (PCL)-rich and (e) nano-hydroxyapatite (nHA)-rich surfaces of the spatially graded meshes. White arrows in E indicate nHA particulates embedded into nanofibers. (Figure was reproduced with the permission from Bayrak et al. [77]).

4.1.3 Cartilage tissue engineering

Other than tendons and ligaments, cartilage tissue is another class of connective tissues that presents elastic behavior and protects the end of bones at joints. Nose, ears, knees, and many other parts of the body contain cartilage tissue. The main ECM components of dense cartilage tissue are collagen and proteoglycans, which are produced by a low number of chondrocytes. After an articular cartilage injury such as rupture, trauma, aging, etc., remodeling and regeneration of the native tissue are challenging due to the low availability of chondrocytes and the complex structure of the tissue. Current approaches are mostly grafts, decellularized structures, microfracture, etc.; however, these approaches pose significant risk to the patient such as inflammation, rejection, implant loosening, or failure.

To repair the damaged articular cartilage, Tuli et al., prepared nanofibrous PCL scaffolds by ES method. The fetal bovine chondrocytes (FBCs) were seeded onto these scaffolds and examined in terms of their ability to maintain chondrocytes in a functional state. According to their results, PCL scaffold seeded with FBC is able to preserve the chondrocyte phenotype by expressing cartilage-specific ECM components such as aggrecan and collagen [78]. In another study, electrospun gelatin/PLA nanofibers were fabricated, and one group was modified by cross-linking with hyaluronic acid to examine the ability to repair cartilage damage. These scaffolds were then subjected to an *in vivo* study on rabbits using an articular cartilage injury model. Results of the *in vivo* studies demonstrated that the hyaluronic-acid-modified scaffolds could increase the repair of cartilage along with their super-absorbent properties and cytocompatibility (**Figure 18**) [79].

Another research group fabricated a scaffold by using coaxial ES with poly (L-lactide-co-caprolactone) and collagen as the shell and kartogenin solution as the

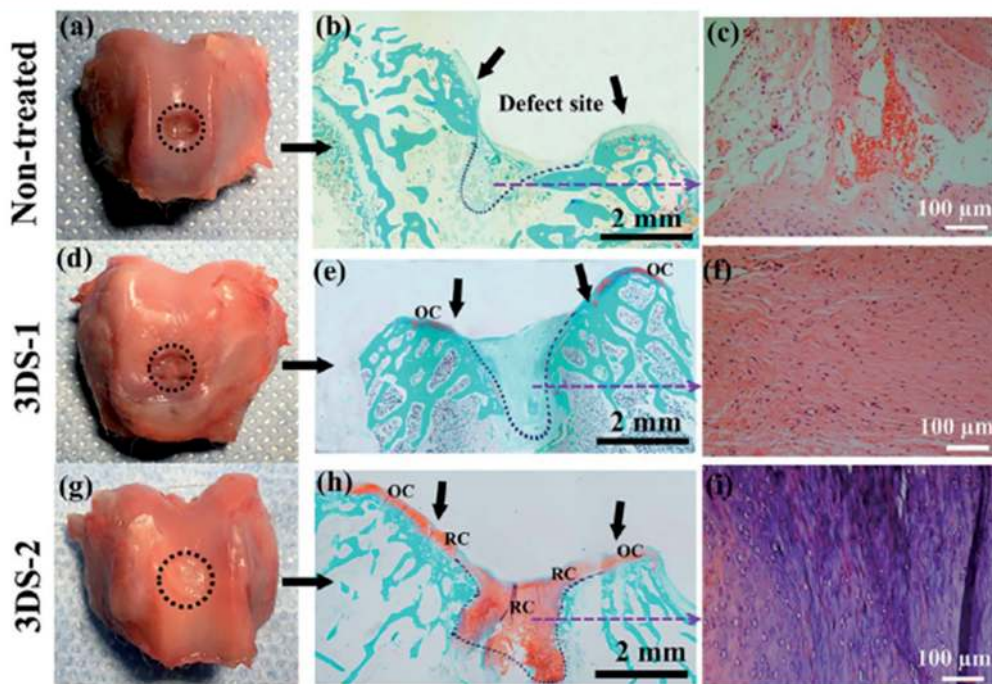


Figure 18. Macroscopic images (a, d, and g) of the cartilage joints from three groups at 12 weeks after surgery. Histological analysis of cartilage defect area from three groups at 12 weeks after surgery, stained with safranin O-fast green (b, e, and h) and H&E (c, f, and i). Arrows and dotted lines indicated the defect sites. (OC: Original cartilage tissue. RC: Repaired cartilage tissue.) (Figure was reproduced with the permission from Chen et al. [79]).

core. Kartogenin's release behavior was monitored over 2 months, and it is shown that the proliferation and chondrogenic differentiation of rabbit bone-marrow-derived MSCs are increased due to the chondrogenesis inducement properties of kartogenin [80]. Furthermore, incorporation of cartilage-derived ECM into nanofibrous scaffolds is another novel way for stimulation of chondrogenic bioactivity [81].

4.2 Skin tissue engineering

The skin is the largest organ in mammals and acts as a physical barrier between the human body and the external environment, which means it is directly exposed to harmful microbial, thermal, mechanical, and chemical damage. Skin tissue, mainly composed of epidermis, dermis, and subcutaneous layer, suffers from integral skin loss with every injury, which can cause functional imbalance in case of large full-thickness skin defects or loss of large skin areas. Skin loss can occur for many reasons, such as disorders, burns, and chronic wounds. For years, autografts and allografts have been used to treat burns or other skin defects, yet the inability of damaged skin tissue to fully heal has opened up the field of tissue engineering for repair broadly to resolve skin-related defects. The basic prerequisite for a material

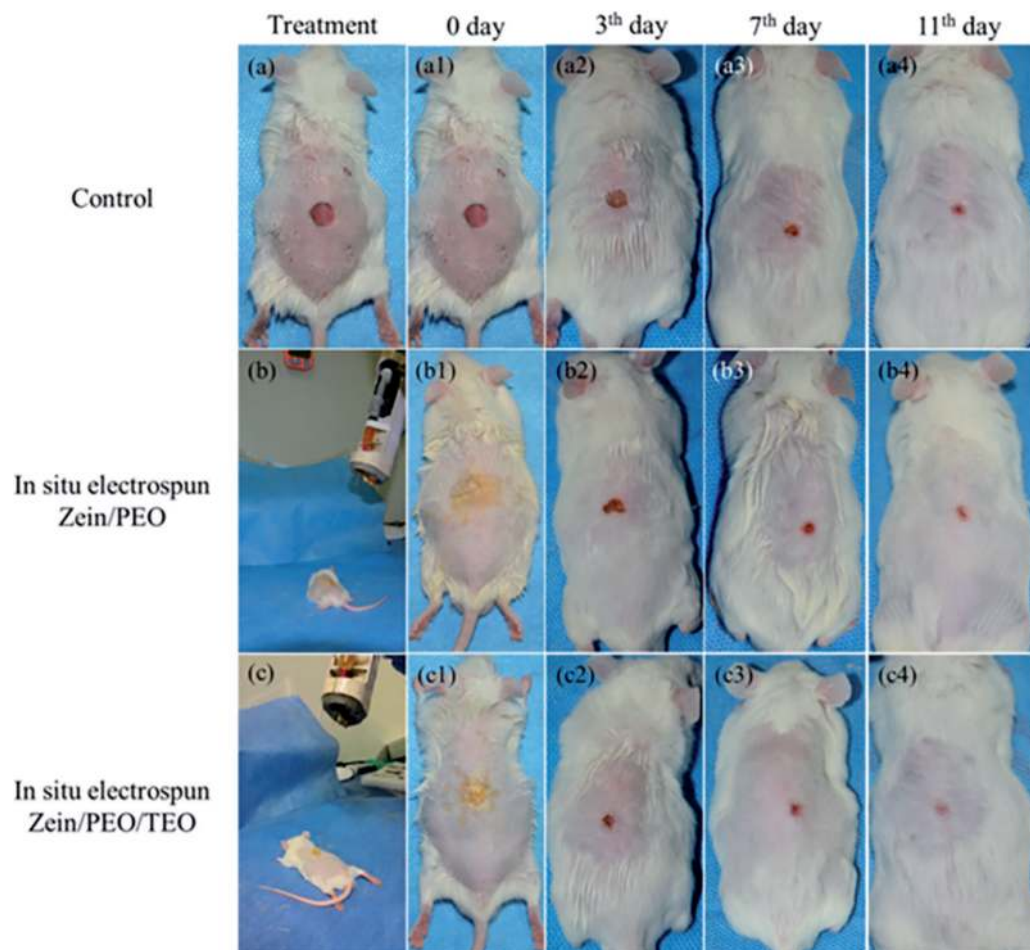


Figure 19. *In situ* deposition of electrospun zein/PEO and zein/PEO/TEO fibrous meshes onto wounds of Kunming mice: (a) no treatment, (b) zein/PEO (control group), and (c) zein/PEO/TEO (study group); gross observation of wounds healing at 0, 3, 7, and 11 days after injury for no treatment (a1–4), zein/PEO (b1–4), and zein/PEO/TEO (c1–4), respectively. (Figure is reproduced with the permission from Liu et al. [87]).

to qualify as a biomaterial is biocompatibility, which is the ability of a material to perform with an appropriate host response [82].

Nanofibrous scaffolds with high porosity can enable cell respiration, infiltration, and absorb exudates. Natural polymers such as chitosan, collagen, and elastin are widely used biomaterials for wound dressing according to their biocompatible and biodegradable properties [83]. Ghosal et al. extracted the silk sericin protein (SS) and blended it with PCL, fabricating a scaffold by using emulsion ES method to examine the effect of the silk sericin protein in the scaffold morphology and proliferation of human primary skin fibroblasts. Results showed an increase in proliferation of the cells on PCL/SS scaffolds [84]. Nanoparticles due to their antioxidant and antibacterial properties are also widely used in this field. Augustine et al. incorporated cerium oxide (CeO_2) nanoparticles into electrospun poly (3-hydroxybutyrate-co-3-hydroxyvalerate) scaffolds and analyzed the wound healing properties. The results showed increased cell proliferation, angiogenesis, and wound healing [85]. Chantre et al., prepared a scaffold by centrifugal ES composed of hyaluronic acid to repair cutaneous tissue. In vitro test showed that due to the high porosity, the infiltration of seeded dermal fibroblasts was successful, and scaffolds present biocompatible and bioactive properties. In vivo studies supported their research as well by the acceleration of the tissue formation, neovascularization, and re-epithelialization [86]. Recently, portable electrospinning devices have been widely used to understand in situ deposition of fibers for wound coverage. This technology allows fibrous scaffolds to form directly on the wound site in a matter of minutes.

For example, Liu et al. fabricated electrospun zein/poly (ethylene oxide) nanofibrous scaffolds modified with thyme essential oil (TEO) by using portable handheld ES device directly onto partial thickness wounds on mice dermal tissue defect (**Figure 19**). It is found that electrospun nanofibers improved the wound healing process within 11 days [87].

4.3 Cardiovascular tissue engineering

Cardiovascular diseases such as coronary artery, cardiomyopathy, hypertension, valve disorders, heart failure, etc., are the leading cause of death globally, and the incidence rates are drastically increasing day by day. Common approach is vascular graft transplantation, but it has some limitations such as lack of organ donors, mismatches, preexisting vascular diseases. These limitations cause a need for more stable, flexible grafts with low toxicity and immunity. Since cardiac tissue ECM causes cardiomyocytes to form into fiber-like cell bundles and these bundles elongate and align themselves, a polymeric scaffold that could mimic this specific feature of cardiac tissue could be a potential candidate for cardiovascular tissue engineering.

To stimulate myocardial regeneration, a 3D PCL-based scaffold with hexagonal structure was fabricated using melt electrowriting method. The aim of the study was to create functional cardiac patches, human induced pluripotent stem cell-derived cardiomyocytes (iPSC-CM) were seeded onto these scaffolds. Results of the in vitro studies showed increased cell alignment, cardiac-maturation-related markers, and sarcomere content. Furthermore, in vivo studies, which are conducted on a contracting porcine heart with a minimally invasive approach, showed that the scaffolds express successful biaxial deformation and also supported high tensile stress [88]. Recently, many studies focus on the development of conductive nanoporous scaffolds for cardiovascular tissue engineering approaches. Bertuoli et al. developed an electrospun conducting and biocompatible uniaxial and core-shell fibers having PLA, PEG, and polyaniline (PAni) for cardiac tissue engineering (**Figure 20**) [89]. They produced PLA, PLA/PAni, and PLA/PEG/PAni fibers and

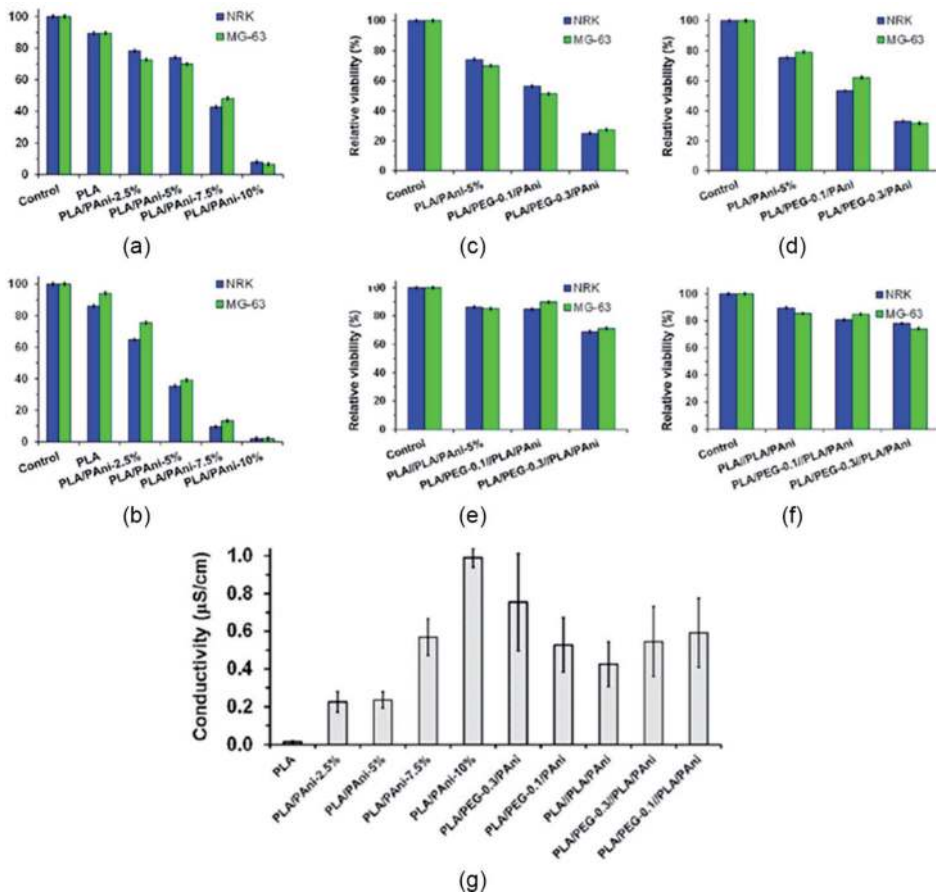


Figure 20. Biocompatibility of PLA/PAni uniaxial fibers expressed as relative viability of normal rat fibroblasts (NRK) and osteosarcoma (MG-63) culture cells onto the fibrous mats after (a) 24 h (cell adhesion) and (b) 96 h (cell proliferation). Biocompatibility of (c, d) PLA/PEG/PAni uniaxial and (e, f) PLA/PEG//PLA/PAni core-shell fibers expressed as relative viability of NRK and MG-63 cells onto the fibrous mats after (c, e) 24 h (cell adhesion) and (d, f) 96 h (cell proliferation). (g) Electrical conductivity of PLA, PLA/PAni, PLA/PEG/PAni, PLA//PLA/PAni, and PLA/PEG//PLA/PAni fibrous mats. (Figures were reproduced with the permission from Bertuoli et al. [89]).

core-shell PLA/PLA/PAni and PLA/PEG//PLA/PAni fibers successfully via uniaxial and coaxial electrospinning, respectively. The proposed PLA/PAni-5% uniaxial and PLA//PLA/PAni coaxial fibers offer very good adhesion for cardiac cells, also being able to modulate cell shape and orientation, something important for the characteristic anisotropy of the cardiac tissue.

Liang et al. fabricated a conductive nanofibrous scaffold by encapsulating polypyrrole (PPY), which is a conductive polymer, in silk fibroin electrospun fibers. Neonatal rat cardiomyocytes (NRCM) and iPSC-CM cells were used to evaluate cardiomyocyte contraction studies. Results showed that both cell lines attached and proliferated onto these scaffolds successfully. Contraction study indicated that scaffolds with different amount of PPY exhibit contraction behavior starting from day 5 [90]. Another group developed a lab-on-a-chip system integrated with PLLA and PU nanofiber mats for cardiovascular diseases. The aim of the study was to create a model of hypoxic myocardial tissue. The microfluidic system allows simultaneously conducting cell cultures under different circumstances. Cardiac cell lines were used for this study, and results showed that cell viability was high, and cells were positioned parallelly on the scaffolds. The hypoxia study indicates that the amount of ATP molecules decreased during biochemical simulation [91].

4.4 Neural tissue engineering

Injuries affecting peripheral or central nervous systems can cause long-lasting loss of neurological functions due to the severity of the injuries. The usual path of an injury is the inhibition of nerve regeneration, which triggers the formation of compact scar tissue at the defect site. The scar tissue inhibits the connection of the axons across the gap, which will result in disruption of the native tissue and signaling pathways. Short nerve injuries, which have less than 20 mm transaction gap between nerves, are usually repaired surgically; however, long-distance nerve defects require nerve healing/regeneration. For long-distance nerve defects, allografts are usually the gold standard, but there are some disadvantages such as limited donor source, nerve size mismatch, neuroma, etc. To overcome these

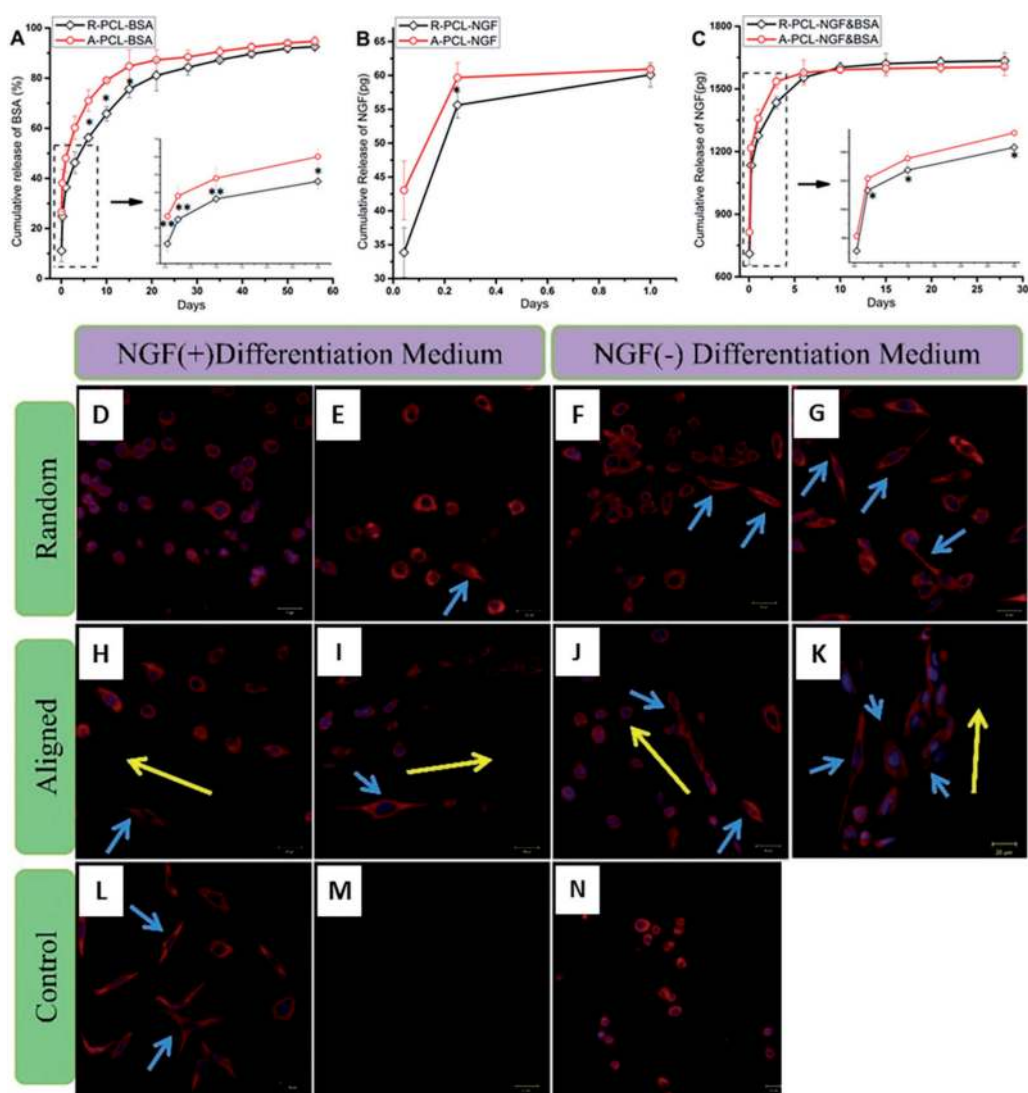


Figure 21.

In vitro release profiles of BSA and NGF. (A) Release curve of BSA from (R/A)-PCL-BSA scaffolds, (B) release properties of NGF from (R/A)-PCL-NGF scaffolds, (C) NGF release from (R/A)-PCL-NGF&BSA scaffolds. Fluorescent images of PC12 cells cultured for 8 days on the surface of different samples with labeling of cytoplasm (red) and nuclei (blue). (D) R-PCL, (E) R-PCL-BSA, (F) R-PCL-NGF, (G) R-PCL-NGF&BSA, (H) A-PCL, (I) A-PCL-BSA, (J) A-PCL-NGF, (K) A-PCL-NGF&BSA, (L) CS-positive, (M) CS-blank for immunofluorescent staining, (N) CS-negative. (yellow arrow indicates the alignment direction for the underlying nanofibers, and blue arrow shows the neurite-bearing PC12 cells.) (Figure was reproduced with the permission from Hu et al. [92]).

challenges, design and fabrication of nerve grafts composed of synthetic or natural polymers are a promising approach for neural tissue engineering.

Nanoporous scaffolds for neural tissue engineering purposes should provide enough surface area for Schwann cells growth and migration, which will direct axons to elongate. Since the orientation structure of axons is axial, some researchers recommended the use of aligned scaffolds, which can provide better contact guidance for cells. Hu et al. fabricated aligned and random PCL scaffolds via ES, and PC-12 (pheochromocytoma of the rat adrenal medulla) neural-like cells were seeded (**Figure 21**).

The results showed that aligned scaffold increased the length of the neurites and directed the extension parallelly to the fiber axis. The study also showed that NGF and bovine serum albumin (BSA) incorporated PCL core-shell nanofibrous scaffolds provide sustained release of NGF and neuronal marker expressions and differentiation of PC-12 cells, which indicates that cells were responded to released NGF [92]. Zhang et al. fabricated a conductive scaffold composed of polyaniline (PAN) and poly (L-lactic-co- ϵ -caprolactone)/silk fibroin nanofibers with incorporation of nerve growth factor (NGF) by using coaxial ES method. The scaffolds successfully support the neurite outgrowth of PC-12 cells, and under electrical stimulation, the amount of neurite-bearing cells and median neurite length were increased [93]. Oxidative stress has a negative impact on nerve cells, so novel approaches, which include antioxidant agents, were investigated. Wang et.al fabricated an antioxidant scaffold composed of lignin/PCL copolymer, and results showed increased mechanical properties of the scaffold and antioxidant activity on cells.

5. Conclusions

The need for less invasive treatment approaches, biocompatible, tailorable, and biodegradable tissue constructs, which can properly mimic native tissues, is still a major challenge for tissue engineering field, and the surface is barely scratched. But nanofibers, due to their tailorable structure, variety of biomaterial options, fabrication routes, and application areas became a popular class of nanomaterials for tissue engineering field. Besides tissue engineering, are other biomedical applications such as drug delivery, biosensor technology, etc. Applications described in this chapter are only a minor proportion of all the results proving the great potential and usefulness of nanofibers. Within this chapter, different fabrication routes, characterization methods, and tissue engineering applications are explained briefly.

Conflict of interest

The authors declare no conflict of interest.

Author details

Ece Bayrak
TOBB University of Economics and Technology, Ankara, Turkey

*Address all correspondence to: ebayrak@etu.edu.tr

IntechOpen

© 2022 The Author(s). Licensee IntechOpen. This chapter is distributed under the terms of the Creative Commons Attribution License (<http://creativecommons.org/licenses/by/3.0>), which permits unrestricted use, distribution, and reproduction in any medium, provided the original work is properly cited. 

References

- [1] Zeleny J. The electrical discharge from liquid points and a hydrostatic method of measuring the electric intensity at their surfaces. *Physical Review*. 1914;**3**:69-91
- [2] Reneker DH, Yarin AL, Fong H, Koombhongse S. Bending instability of electrically charged liquid jets of polymer solutions in electrospinning. *Journal of Applied Physics*. 2000;**87**: 4531-4547
- [3] Baumgarten PK. Electrostatic spinning of acrylic microfibers. *Journal of Colloid and Interface Science*. 1971;**36**:71-79
- [4] Bharwaj N, Kundu SC. Electrospinning: A fascinating fiber fabrication techniques. *Biotechnology Advances*. 2010;**28**(3):325-347
- [5] Gugulothu D, Barhoum A, Nerella R, Ajmer R, Bechlyan M. Fabrication of nanofibers: Electrospinning and non-electrospinning techniques. In: *Handbook of Nanofibers*. Switzerland: Springer Cham; 2018. pp. 1-34
- [6] Huang ZM, Zhang YZ, Kotaki M, Ramakrishna S. A review on polymer nanofibers by electrospinning and their applications in nanocomposites. *Composites Science and Technology*. 2003;**63**(15):2223-2253
- [7] Gonçalves AM, Moreira A, Weber A, Williams GR, Costa PF. Osteochondral tissue engineering: The potential of electrospinning and additive manufacturing. *Pharmaceutics*. 2021;**13**(7):983
- [8] Ura DP, Rosell-Llompert J, Zaszczynska A, Vasilyev G, Gradys A, Szewczyk PK, et al. The role of electrical polarity in electrospinning and on the mechanical and structural properties of as-spun fibers. *Materials*. 2020;**13**(18):4169
- [9] Wu YK, Wang L, Fan J, Shou W, Zhou BM, Liu Y. Multi-jet electrospinning with auxiliary electrode: The influence of solution properties. *Polymers*. 2018;**10**(6):572
- [10] Li WJ, Shanti RM, Tuan RS. Electrospinning Technology for Nanofibrous Scaffolds in tissue engineering. In: Kumar CSSR, editor. *Nanotechnologies for the Life Sciences*. 1st ed. Weinheim: Wiley; 2007. pp. 135-187. DOI: 10.1002/9783527610419.ntls0097
- [11] Haider A, Haider S, Kang IK. A comprehensive review summarizing the effect of electrospinning parameters and potential applications of nanofibers in biomedical and biotechnology. *Arabian Journal of Chemistry*. 2018;**8**:1165-1188
- [12] Migliaresi C, Ruffo GA, Volpato FZ, Zeni D. Advanced electrospinning setups and special fibre and mesh morphologies. In: Neves NM, editor. *Electrospinning for Advanced Biomedical Applications and Therapies*. 1st ed. United Kingdom: Smithers Rapra; 2012. pp. 22-68
- [13] Yoon J, Yang HS, Lee BS, Yu WR. Recent progress in coaxial electrospinning: New parameters, various structures and wide applications. *Advanced Materials*. 2018;**30**(42):1704765
- [14] Brown TD, Dalton PD, Hutmacher DW. Melt electrospinning today: An opportune time for an emerging polymer process. *Progress in Polymer Science*. 2016;**56**:116-166
- [15] Taghavi SM, Larson RG. Regularized thin-fiber model for nanofiber formation by centrifugal spinning. *Physical Review E*. 2014;**89**(2):023011
- [16] Blachowicz T, Ehrmann A. Most recent developments in electrospun

- magnetic nanofibers: A review. *Journal of Engineered Fibers and Fabrics*. 2020;**15**:1558925019900843
- [17] Yoon YI, Park KE, Lee SJ, Park WH. Fabrication of microfibrinous and nanofibrinous scaffolds: Melt and hybrid electrospinning and surface modification of poly(L-lactic acid) with plasticizer. *BioMed Research International*. 2013;**2013**:309048. DOI: 10.1155/2013/309048
- [18] Zhang LH, Duan XP, Yan X, Yu M, Ning X, Zhao Y, et al. Recent advances in melt electrospinning. *RSC Advances*. 2016;**6**(58):53400-53414
- [19] Zhang X, Lua Y. Centrifugal spinning: An alternative approach to fabricate nanofibers at high speed and low cost. *Polymer Reviews*. 2014;**54**:677-107
- [20] Loordhuswamy AM, Krishnaswamy VR, Korrapati PS, Thinakaran S, Rengaswami GDV. Fabrication of highly aligned fibrous scaffolds for tissue regeneration by centrifugal spinning technology. *Materials Science and Engineering: C*. 2014;**42**:799-807
- [21] Xu J, Liu X, Zhang Z, Wang L, Tan R, Zhang D. Controllable generation of nanofibers through a magnetic-field-assisted electrospinning design. *Material Letters*. 2019;**247**:19-24
- [22] Liu Y, Zhang X, Xia Y, Yang H. Magnetic-field-assisted electrospinning of aligned straight and wavy polymeric nanofibers. *Advanced Materials*. 2010;**22**:2454-2457
- [23] Li T'T, Yan M, Xu W, Shiu BC, Lou CW, Lin JH. Mass-production and characterizations of polyvinyl alcohol/sodium alginate/graphene porous nanofiber membranes using needleless dynamic linear electrospinning. *Polymers*. 2018;**10**(10):1167
- [24] Nikmaram N, Roohinejad S, Hashemi S, Koubaa M, Barba FJ, Abbaspourrad A, et al. Emulsion-based systems for fabrication of electrospun nanofibers: Food, pharmaceutical and biomedical applications. *RSC Advances*. 2017;**7**(46):28951-28964
- [25] Niu H, Lin T. Fiber generators in needleless electrospinning. *Journal of Nanomaterials*. 2012;**12**:1-13
- [26] Partheniadis I, Nikolakakis O, Laidmæ I, Heinamaki J. A mini-review: Needleless electrospinning of nanofibers for pharmaceutical and biomedical applications. *PRO*. 2020;**8**(6):673
- [27] Buzgo M, Mickova A, Rampickova M, Doupanik M. Blend electrospinning, coaxial electrospinning, and emulsion electrospinning techniques. In: Tampieri A, Focarete ML, editors. *Core-Shell Nanostructures for Drug Delivery and Theranostis*. 1st ed. Sawston, UK: Woodhead Publishing, Elsevier; 2018. pp. 325-347
- [28] Zhang X, Shi X, Gautrot JE, Peijs T. Nanoengineered electrospun fibers and their biomedical applications: A review. *Nano*. 2021;**7**(1):1-34
- [29] Arafat MT, Tronci G, Yin J, Wood DJ, Russell SJ. Biomimetic wet-stable fibres via wet spinning and diacid-based crosslinking of collagen triple helices. *PRO*. 2015;**77**:102-112
- [30] Wang L, Lundahl MJ, Greca LG, Papageorgiou AC, Borghei M, Rojas OJ. Effects of non-solvents and electrolytes on the formation and properties of cellulose I filaments. *Scientific Reports*. 2019;**9**(1):1-11
- [31] Puppi D, Chiellini F. Wet-spinning of biomedical polymers: From single fibre production to additive manufacturing of three-dimensional scaffolds. *Polymer International*. 2017;**66**(12):1690-1696

- [32] Ramakrishna S, Fujihara K, Teo WE, Lim TK, Ma Z. *An Introduction to Electrospinning and Nanofibers*. 1st ed. Singapore: World Scientific Press; 2005. p. 10
- [33] Ondarcuhu T, Joachim C. Drawing a single nanofibre over hundreds of microns. *Euromphysics Letters*. 1998;**42**(2):215
- [34] Wang J, Nain AS. Suspended micro/nanofiber hierarchical biological scaffolds fabricated using non-electrospinning STEP technique. *Langmuir*. 2014;**30**:13641-13649
- [35] Wng Y, Zheng M, Lu H, Feng S, Ji G, Cao J. Template synthesis of carbon nanofibers containing linear mesocage arrays. *Nanoscale Research Letters*. 2010;**5**(6):913-916
- [36] Liu S, Shan H, Xia S, Yan J, Ding B. Polymer template synthesis of flexible SiO₂ nanofibers to upgrade composite electrolytes. *ACS Applied Materials & Interfaces*. 2020;**12**(28):31439-31447
- [37] Ma PX, Zhang R. Synthetic nano-scale fibrous extracellular matrix. *Journal of Biomedical Materials Research Part A*. 1999;**46**:60-72
- [38] Zhang R, Ma PX. Processing polymer scaffolds: Phase separation. In: Atala A, Lanza R, Lanza RP, editors. *Methods of Tissue Engineering*. 1st ed. San Diego: Academic Press; 2002. pp. 715-724
- [39] Sharma J, Lizu M, Stewart M, Zygula K, Lu Y, Chauhan R, et al. Multifunctional nanofibers towards active biomedical therapeutics. *Polymers*. 2015;**7**(2):186-219
- [40] Xu XD, Jin Y, Liu Y, Zhang XZ, Zhuo RX. Self-assembly behavior of peptide amphiphiles (PAs) with different length of hydrophobic alkyl tails. *Colloids and Surfaces B: Biointerfaces*. 2010;**81**(1):329-335
- [41] Wang L, Gong C, Yuan X, Wei G. Controlling the self-assembly of biomolecules into functional nanomaterials through internal interactions and external stimulations: A review. *Nanomaterials*. 2019;**9**(2):285
- [42] Raaijmakers MJ, Benes NE. Current trends in interfacial polymerization. *Progress in Polymer Science*. 2016;**63**:86-142
- [43] Huang J, Kaner RB. A general chemical route to polyaniline nanofibers. *Journal of the American Chemical Society*. 2004;**126**(3):851-855
- [44] Freitas TV, Sousa EA, Fuzari GC Jr, Arlindo EP. Different morphologies of polyaniline nanostructures synthesized by interfacial polymerization. *Materials Letters*. 2018;**224**:42-45
- [45] Sirc J, Hobzova R, Kostina N, Munzarova M, Juklickova M, Lhotka M, et al. Morphological characterization of nanofibers: Methods and application in practice. *Journal of Nanomaterials*. 2012;**2012**:327369. DOI: 10.1155/2012/327369
- [46] Oliviera JE, Mattoso LH, Orts WJ, Medeiros ES. Structural and morphological characterization of micro and nanofibers produced by electrospinning and solution blow spinning: A comparative study. *Advances in Materials Science and Engineering*. 2013. DOI: 10.1155/2013/409572
- [47] Megelski S, Stephens JS, Chase DB, Rabolt JF. Micro- and nanostructured surface morphology on electrospun polymer fibers. *Macromolecules*. 2002;**35**(22):8456-8466
- [48] Deng X, Xiong F, Li X, Xiang B, Li Z, Wu X, et al. Application of atomic force microscopy in cancer research. *Journal of Nanobiotechnology*. 2018;**16**(1):1-15
- [49] Birdi KS. *Scanning Probe Microscopes: Applications in Science*

and Technology. 1st ed. London: CRC Press, Taylor & Francis Group; 2003. p. 16. DOI: 10.1201/9780203011072

[50] Kaur H, Bhagwat SR, Sharma TK, Kumar A. Analytical techniques for characterization of biological molecules–proteins and aptamers/oligonucleotides. *Bioanalysis*. 2019;**11**(02):103-117

[51] Bunaciu AA, Udristioiu EG, Aboul-Enein HY. X-ray diffraction: Instrumentation and applications. *Critical Reviews in Analytical Chemistry*. 2015;**45**(4):289-299

[52] Loganathan S, Valapa RB, Mishra RK, Pugazhenti G, Thomas S. Thermogravimetric analysis for characterization of nanomaterials. In: Thomas S, Thomas R, Zachariah A, Mishra R, editors. *Thermal and Rheological Measurement Techniques for Nanomaterials Characterization*. 1st ed. Elsevier; 2017. pp. 67-108

[53] Coats AW, Redfern JP. Thermogravimetric analysis. A review. *Analyst*. 1963;**88**(1053):906-924

[54] Saadatkhan N, Carillo Garcia A, Ackermann S, Leclerc P, Latifi M, Samih S, et al. Experimental methods in chemical engineering: Thermogravimetric analysis-TGA. *The Canadian Journal of Chemical Engineering*. 2020;**98**(1):34-43

[55] Zhou J, Cai Q, Liu X, Ding Y, Xu F. Temperature effect on the mechanical properties of electrospun PU nanofibers. *Nanoscale Research Letters*. 2018;**13**(1):1-5

[56] Tan EPS, Lim CT. Mechanical characterization of nanofibers. *Composites*. 2006;**66**(9):1102-1111

[57] Seyama H, Soma M, Theng BKG. X-ray photoelectron spectroscopy. In: Bergaya F, Lagaly G, editors. *Developments in Clay Science*. 1st ed.

Amsterdam, Netherlands: Elsevier; 2013. pp. 161-176

[58] Lee SH, Park SM, Lee LP. Optical methods in studies of olfactory system. In: Park T, editor. *Bioelectronic Nose*. Dordrecht: Springer; 2014. pp. 191-220

[59] Seah MP. Quantitative AES and XPS: Convergence between theory and experimental databases. *Journal of Electron Spectroscopy and Related Phenomena*. 1999;**100**:55-73

[60] Polini A, Yang F. Physicochemical characterization of nanofiber composites. In: Ramalingam M, Ramakrishna S, editors. *Nanofiber Composites for Biomedical Applications*. 1st ed. Sawston, UK: Woodhead Publishing, Elsevier; 2017. pp. 97-115

[61] Kim HH. Endoscopic Raman spectroscopy for molecular fingerprinting of gastric cancer: Principle to implementation. *BioMed Research International*. 2015; **2015**:670121. DOI: 10.1155/2015/670121

[62] Titus D, Samuel EJJ, Roopan SM. Nanoparticle characterization techniques. In: Kumar Shukla A, Iravani S, editors. *Green Synthesis, Characterization and Applications of Nanoparticles*. 1st ed. Amsterdam: Elsevier; 2019. pp. 303-319

[63] de Melo Pereira D, Habibovic P. Biomineralization-inspired material Design for Bone Regeneration. *Advanced Healthcare Materials*. 2018;**7**(22):1800700

[64] Silber J, Anderson DG, Daffner SD, Brislin BT, Leland JM, Hilibrand AS, et al. Donor site morbidity after anterior iliac crest bone harvest for single-level anterior cervical discectomy and fusion. *Spine*. 2003;**28**(2):134-139

[65] Mankin HJ, Hornicek FJ, Raskin KA. Infection in massive bone allografts.

Clinical Orthopaedics and Related Research. 2005;**432**:210-216

[66] Du Y, Guo JL, Wang J, Mikos AG, Zhang S. Hierarchically designed bone scaffolds: From internal cues to external stimuli. *Biomaterials*. 2019;**218**:119334

[67] Cai YZ, Zhang GR, Wang LL, Jiang YZ, Ouyang HW, Zou XH. Novel biodegradable three-dimensional macroporous scaffold using aligned electrospun nanofibrous yarns for bone tissue engineering. *Journal of Biomedical Materials Research Part A*. 2012;**100**(5):1187-1194

[68] Nedjari S, Awaja F, Altankov G. Three dimensional honeycomb patterned fibrinogen based nanofibers induce substantial osteogenic response of mesenchymal stem cells. *Scientific Reports*. 2017;**7**(1):1-11

[69] Abdal-hay A, Abbasi N, Gwiazda M, Hamlet S, Ivanovski S. Novel polycaprolactone/hydroxyapatite nanocomposite fibrous scaffolds by direct melt-electrospinning writing. *European Polymer Journal*. 2018;**105**: 257-264

[70] Velioglu ZB, Pulat D, Demirbakan B, Ozcan B, Bayrak E, Erisken C. 3D-printed poly (lactic acid) scaffolds for trabecular bone repair and regeneration: Scaffold and native bone characterization. *Connective Tissue Research*. 2019;**60**(3):274-282

[71] Lukášová V, Buzgo M, Vocetková K, Sovková V, Doupník M, Himawan E, et al. Needleless electrospun and centrifugal spun poly- ϵ -caprolactone scaffolds as a carrier for platelets in tissue engineering applications: A comparative study with hMSCs. *Materials Science and Engineering: C*. 2019;**97**:567-575

[72] Olender E, Uhrynowska-Tyszkiewicz I, Kaminski A. Revitalization of biostatic tissue

allografts: New perspectives in tissue transplantology. In *Transplantation Proceedings*. 2011;**43**(8):3137-3141

[73] Yang G, Lin H, Rothrauff BB, Yu S, Tuan RS. Multilayered polycaprolactone/gelatin fiber-hydrogel composite for tendon tissue engineering. *Acta Biomaterialia*. 2016;**35**:68-76

[74] Perikamana SKM, Lee J, Ahmad T, Kim EM, Byun H, Lee S, et al. Harnessing biochemical and structural cues for tenogenic differentiation of adipose derived stem cells (ADSCs) and development of an in vitro tissue interface mimicking tendon-bone insertion graft. *Biomaterials*. 2018;**165**:79-93

[75] Rinoldi C, Kijeńska E, Chlanda A, Choinska E, Khenoussi N, Tamayol A, et al. Nanobead-on-string composites for tendon tissue engineering. *Journal of Materials Chemistry B*. 2018;**6**(19): 3116-3127

[76] Chen CH, Li DL, Chuang ADC, Dash BS, Chen JP. Tension stimulation of tenocytes in aligned hyaluronic acid/platelet-rich plasma-Polycaprolactone Core-sheath nanofiber membrane scaffold for tendon tissue engineering. *International Journal of Molecular Sciences*. 2021;**22**:11215

[77] Bayrak E, Ozcan B, Erisken C. Processing of polycaprolactone and hydroxyapatite to fabricate graded electrospun composites for tendon-bone interface regeneration. *Journal of Polymer Engineering*. 2017;**37**(1):99-106

[78] Tuli R, Li WJ, Tuan RS. Current state of cartilage tissue engineering. *Arthritis Research & Therapy*. 2003;**5**(5):1-4

[79] Chen W, Chen S, Morsi Y, El-Hamshary H, El-Newhy M, Fan C, et al. Superabsorbent 3D scaffold based on electrospun nanofibers for cartilage tissue engineering. *ACS Applied Materials & Interfaces*. 2016;**8**(37):24415-24425

- [80] Yin H, Wang J, Gu Z, Feng W, Gao M, Wu Y, et al. Evaluation of the potential of kartogenin encapsulated poly (L-lactic acid-co-caprolactone)/ collagen nanofibers for tracheal cartilage regeneration. *Journal of Biomaterials Applications*. 2017;**32**(3): 331-341
- [81] Garrigues NW, Little D, Sanchez-Adams J, Ruch DS, Guilak F. Electrospun cartilage-derived matrix scaffolds for cartilage tissue engineering. *Journal of Biomedical Materials Research Part A*. 2014;**102**(11):3998-4008
- [82] Borena BM, Martens A, Broeckx SY, Meyer E, Chiers K, Duchateau L. Regenerative skin wound healing in mammals: State-of-the-art on growth factor and stem cell based treatments. *Cellular Physiology and Biochemistry*. 2015;**36**:1-23
- [83] Demir M, Büyükserin F, Bayrak E, Türker NS. Development and characterization of metronidazole-loaded and chitosan-coated PCL electrospun Fibres for potential applications in guided tissue regeneration. *Trends in Biomaterials & Artificial Organs*. 2021;**35**(3):255-263
- [84] Ghosal K, Manakhov A, Zajíčková L, Thomas S. Structural and surface compatibility study of modified electrospun poly (ϵ -caprolactone) (PCL) composites for skin tissue engineering. *AAPS PharmSciTech*. 2017;**18**(1):72-81
- [85] Augustine R, Hasan A, Patan NK, Dalvi YB, Varghese R, Antony A, et al. Cerium oxide nanoparticle incorporated electrospun poly (3-hydroxybutyrate-co-3-hydroxyvalerate) membranes for diabetic wound healing applications. *ACS Biomaterials Science & Engineering*. 2019;**6**(1):58-70
- [86] Chantre CO, Gonzalez GM, Ahn S, Cera L, Campbell PH, Hoerstrup SP, et al. Porous biomimetic hyaluronic acid and extracellular matrix protein nanofiber scaffolds for accelerated cutaneous tissue repair. *ACS Applied Materials & Interfaces*. 2019;**11**(49):45498-45510
- [87] Liu JX, Dong WH, Mou XJ, Liu GS, Huang XW, Yan X, et al. In situ electrospun zein/thyme essential oil-based membranes as an effective antibacterial wound dressing. *ACS Applied Biomaterials*. 2019;**3**(1):302-307
- [88] Castilho M, van Mil A, Maher M, Metz CH, Hochleitner G, Groll J, et al. Melt electrowriting allows tailored microstructural and mechanical design of scaffolds to advance functional human myocardial tissue formation. *Advanced Functional Materials*. 2018;**28**(40):1803151
- [89] Bertuoli PT, Ordone J, Armelin E, Perez-Amodio S, Baldissera AF, Ferreira CA, et al. Electrospun conducting and biocompatible uniaxial and Core-Shell fibers having poly(lactic acid), poly(ethylene glycol), and polyaniline for cardiac tissue engineering. *ACS Omega*. 2019;**4**: 3660-3672
- [90] Liang Y, Mitriashkin A, Lim TT, Goh JCH. Conductive polypyrrole-encapsulated silk fibroin fibers for cardiac tissue engineering. *Biomaterials*. 2021;**276**:121008
- [91] Kobuszewska A, Kolodziejek D, Wojasinski M, Jastrzebska E, Ciach T, Brzozka Z. Lab-on-a-chip system integrated with nanofiber mats used as a potential tool to study cardiovascular diseases (CVDs). *Sensors and Actuators B: Chemical*. 2021;**330**: 129291
- [92] Hu J, Tian L, Prabhakaran MP, Ding X, Ramakrishna S. Fabrication of nerve growth factor encapsulated aligned poly (ϵ -caprolactone) nanofibers and their assessment as a

potential neural tissue engineering
scaffold. *Polymers*. 2016;**8**(2):54

[93] Zhang J, Qiu K, Sun B, Fang J,
Zhang K, Hany EH, et al. The aligned
core–sheath nanofibers with electrical
conductivity for neural tissue
engineering. *Journal of Materials
Chemistry B*. 2014;**2**(45):7945-7954